Ben-Gurion University of the Negev

Jacob Blaustein Institutes for Desert Research

Albert Katz International School for Desert Studies

Monitoring and Predicting Forest Phenology by Multispectral Remote Sensing Techniques

Thesis submitted in partial fulfillment of the requirements for the degree of "Master of Arts"

By: Alexandra Shtein

October 2015

Ben-Gurion University of the Negev

Jacob Blaustein Institutes for Desert Research

Albert Katz International School for Desert Studies

Monitoring and Predicting Forest Phenology by Multispectral Remote Sensing Techniques

Thesis submitted in partial fulfillment of the requirements for the degree of “Master of Arts”

By: Alexandra Shtein

Under the Supervision of Prof. Arnon Karnieli

Department of Solar Energy and Environmental Physics

Author's Signature ………… ………………… Date Sep. 27, 2015

Approved by the Supervisor…. ….………………… Date Sep. 22, 2015

Approved by the Director of the school ………………. Date …………….

Abstract

Phenology is the study of recurring life-cycle events that are initiated and driven by environmental factors. Changes in plant phenology constitute solid evidence for the influence of global climate change on different species and ecosystems, therefore, it is highly important to monitor phenology and study the effect of climate variability on it. Previous phenological studies focused mainly on exploring the shifts in the timing of phenological events as a response to various climatic changes. Another developing research field is phenology modeling using climatic factors for explanatory and predictive purposes. In the framework of phenology monitoring, the main applied methodology was ground based observations and simple web RGB cameras. Although multi spectral cameras allow the utilization of common used vegetation indices for monitoring purposes, they were rarely used for phenology monitoring. The objectives of this research were twofold: (1) Exploring the relations between three main growth limiting factors (precipitation, temperature and radiation) and two vegetation indices (normalized difference vegetation index (NDVI) and normalized difference water index (NDWI)) in four forests located along a climatic gradient in Israel. (2) Monitoring the phenological cycle of four Mediterranean tree species using Multi spectral camera in Ramat HaNadiv Park.

Within the framework of phenological modeling, NDVI and NDWI were used as a proxy to the phenology of the forests. Statistical time series modeling approach was used in order to establish best explanatory model. This analysis showed the decreasing influence of precipitation as a limiting factor from the southern arid site to the northern dry sub-humid site; in the southern Yatir site precipitation was the main factor dictating the phenology of the forest. However, in the three others sites (Jerusalem corridor, Carmel and Galilee) the influence of temperature and radiation on phenology was either similar to that of the precipitation or higher. The explanatory power of the models that were fitted for each site was relatively high ranging from adjusted R^2 results of 0.76 to 0.87 for the NDVI, and 0.67 to 0.84 for the NDWI (depending on the site). Predictive abilities of the models were tested on a validation period and showed reasonable functioning, with lower measures in years with extreme climatic events.

For phenological monitoring, monthly NDVI time series were retrieved from the multi spectral camera. Alongside, seasonal physiological measurements were conducted to support the observed phenological processes. NDVI time series showed cycles that are typical for evergreen Mediterranean tree species, with higher values around spring season. Physiological measurements indicated on water deficit due to the long dry spell in the summer months. No significant correlation was found between chlorophyll concentrations and NDVI values.

In summary, statistical phenology modeling approach can provide good explanatory performance, reflecting the constraints of climatic variables on phenology. The prediction abilities of such models showed reasonable function, and should be further studied in order to be useful for the prediction of phenological events. Phenological monitoring project in Ramat HaNadiv showed the feasibility of a new potential methodological tool; however several technical and methodological aspects should be further studied.

Acknowledgments

I would like to express my deep gratitude to my supervisor Professor Arnon Karnieli for giving me the chance of being part of this fascinating project. His door was always open for any question, consultation, and dilemma. I would also like to thank deeply to all the people that made this project possible: Our deer lab members for their help, support and advices, our lab technician Sasha Goldberg for his enormous help in our the intensive field days and in general with any technical problem, Dr. Golan Bel for the statistical consultation, Dr. Natalya Panov for her professional advices, Paivi Yuval for sharing her experience and knowledge with me and for her great help during the field work, Dr. Jose Gruenzweig for his help with the tree selection in Ramat HaNadiv site, Ramat Hanadiv staff (Dr. Liat Hadar, Hasan, Albert and Dudu) for their help and support during this project, Dr. Yagil Osem for providing detailed information about tree species composition within the forests, and Professor Uriel Safriel for providing the aridity index map.

Table of Contents

List of Figures

List of Tables

1. Introduction

1.1 Plant Phenology and climate change

Phenology can be defined as the study of recurring life-cycle events that are initiated and driven by environmental factors (Morisette et al., 2009). In the context of plants, green-up, maturity, senescence, and dormancy are examples of phenological events. Phenology constitutes a major aspect of tree functioning, productivity, and even its survival depends on the ability to adjust pheno-phases timing to changing climatic conditions (Kramer, Leinonen, & Loustau, 2000). The impacts of changing phenology can be vast, ranging from local influences on agriculture, fisheries, forestry, and public health (Zhao et al., 2013) and up to influences on global net carbon uptake (Churkina, Schimel, Braswell, & Xiao, 2005). Phenology is valuable also for climate change research as it serves as a “fingerprint” of occurring climatic changes (Parmesan & Gary, 2003). Forests are interesting and important ecosystems for phenological monitoring, due to their extensive global cover, their long life span, and their functioning as carbon storing ecosystems.

In recent decades and in different regions worldwide, forests have experienced dry periods that have led large-scale decline and even tree mortality (Allen et al., 2010). It was also shown that such dry periods trigger various phenological changes (Estiarte & Peñuelas, 2015; Kuster, Dobbertin, Günthardt-Goerg, Schaub, & Arend, 2014; Misson et al., 2011). Future scenarios show alterations in climate regime along with the increase in the frequency and intensity of extreme climatic events such as droughts, fires, storms, and floods (IPCC, 2014). Climatic drying trends have been observed also across the Mediterranean area (Kafle & Bruins, 2009), and further drying trends associated with reduced precipitation and increased evaporative demand are expected (Cook, Smerdon, Seager, & Coats, 2014). In this area, where water availability is a main limiting growth factor (Kramer et al., 2000), forests may be subjected to the negative influences of future drought periods. In Israel, planted and natural forests are spread along a sharp climatic gradient, as defined by the aridity index (Fig. 1), from arid in the southern parts of it, through semi-arid in the center and up to dry sub humid and humid in the northern parts.

Although the influence of drought events on forested areas in Israel had been studied before (e.g., Dorman et al., 2013a, 2013b; Volcani et al., 2005), there are still some uncertainties about how climate in the last decades has influenced the phenology of these forests. Specifically, it is still unclear how important particular climatic factors are in determining forest phenology, and what is the ability to predict future phenological cycles from climatic variables. These questions can be addressed by establishing models that quantify the impact of climate variables on phenological cycles.

1.2 Plant phenology modeling

Previous phenological studies focused mainly on exploring the shifts in the timing of phenological events as a response to various climatic changes, as these shifts constitute solid evidence of the influence of global climate change on different species and ecosystems (Cleland, Chiariello, Loarie, Mooney, & Field, 2006). Such alternations include the effect of increasing temperatures (Luedeling, Guo, Dai, Leslie, & Blanke, 2013), shifting precipitation (Nagy, Kreyling, Gellesch, Beierkuhnlein, & Jentsch, 2013), and rising CO_2 concentrations (Johnston and Reekie, 2008; Zelikova et al., 2015) on plant phenology. Another developing research field is phenology modeling using climatic variables. Through the quantification of the relations between climate and phenology in previous years, predictions of future phenological cycles can be achieved. In this framework, many different phenology models were established in the last decades. These models range from simple to complex ones, depending on the amount of species, predictors, assumptions, and their spatial scale. Zhao et al. (2013) suggested dividing the existing plant phenology models to three main modeling approaches: statistical, mechanistic, and theoretical models.

The first type of modeling approach includes the statistical or empirical models that correlate the timing of phenological events to different environmental factors, mainly climatic variables. Some of the models rely on the simplifying assumption of linear correlations between phenological events and climatic factors (Zhao et al., 2013). For instance, least-squares regression was used to quantify the response of flowering timing and duration to the surface temperature and the amount of precipitation (Nagy et al., 2013). Other, more complex, statistical models assumed that certain amount of heat, photoheat or hydro-heat units above a certain threshold is needed to provoke the occurrence of specific phenological event (Zhao et al., 2013). Examples for such models are the spring warming model, winter chilling and spring warming model, and photo-thermal model (Hunter & Lechowicz, 1992). An obvious advantage of this approach lies in its simplified calculation procedures and the availability of the inputs. On the other hand, this simplicity can be also a disadvantage, since specific biological processes are not being considered. Moreover, these models were implemented in limited regions, on small sets of events and plants, and their implications and predictive abilities were relatively restricted (Zhao et al., 2013).

The second type is the mechanistic modeling approach that describes known or assumed cause-effect relationships between biological processes (e.g. bud burst, dormancy, onset, and cessation of the growth) and key driving variables present in the environment of plants (e.g. soil water availability, photoperiodic cues, and mean temperature) (Zhao et al., 2013). These models make assumptions about the actual physiological processes of plant development. Onset models, which aim to simulate the start of the growing season, are one example for mechanistic models (Chuine, 2000). They are based on the response of bud growth to forcing temperatures (temperatures that force growth during spring when dormancy has been released) or to chilling temperatures (temperatures that break dormancy) (Chuine, 2000). Although the mechanistic approach considers different growth promoting factors and triggering events, there are still mechanism uncertainties due to lack of direct measurements of the state of development during the physical processes (Zhao et al., 2013).

Among these mechanistic phenological models, relatively few studies aimed to predict phenology responses to climate change scenarios. The mechanistic process-based forest model that was used by Kramer et al. (2000) aimed to give such a prediction in order to evaluate the effect of different climate change scenarios on the growth of different forests. Their model showed that in the Mediterranean forests, the response of growth to significant drought is species-dependent. Specifically, this climatic event is predicted to a have a negative effect for several years on the leaf area index of *Pinus pinaster* species. Another mechanistic model (Vitasse et al., 2011) aimed to predict seasonal shifts in phenological events for the 21st century in response to climate warming in European temperate trees. Their models were tested and validated on 2-3 years of direct phenological observations. Although observations were taken from an elevation gradient that explored a temperature range, such limited dataset can restrict the validity of the predictive model. Improvements in this matter can be achieved by using long-term datasets from remote sensing observations.

The third type is the theoretical models that attempt to model various aspects of plant physiology (Zhao et al., 2013). Remote sensing-based phenology model is an important example for this type of models. In contrast to traditional techniques of phenology monitoring, remote sensing data from various sensors aboard satellite platforms allows to observe and monitor phenology over large scales and at regular intervals (Ganguly, Friedl, Tan, Zhang, & Verma, 2010). This modeling approach uses satellite vegetation indices (VIs) data and methods for optimizing the model parameters (Zhao et al., 2013). VIs are based on relations between certain spectral bands and are often used to quantify vegetation phenological and physiological state. The normalized difference vegetation index (NDVI) and normalized difference water index (NDWI) are examples for widely-used VIs, that were implemented previously to monitor vegetation response to climate (Anderson et al., 2010; Carcinoid, Liver, Nodes, Metastases, & Responded, 2010; Gu, Brown, Verdin, & Wardlow, 2007). These VIs were also widely used for phenological monitoring and assessment of climate influence on plant phenology (e.g. Delbart et al. 2005, White et al. 2005, Pio et al. 2006, Hermance et al. 2015). VIs are good indicators for the phenology of plants, as they reflect changes in physiological aspects associated with phenological changes. NDVI is a spectral index based on the relations between maximal reflectance in the near infrared region due to leaf internal structure, and minimal reflectance in the red spectral region due to chlorophyll absorption (Tucker, 1979):

$$NDVI = \frac{\rho NIR - \rho RED}{\rho NIR + \rho RED} \quad (1)$$

Where *ρNIR* and *ρRED* are the reflectance values in the near infrared and red spectral regions, respectively. This index, which is tuned to sense changes in leaf structure and chlorophyll content (Tucker, 1979), has been used successfully to estimate 'greenness', above ground net primary productivity, leaf area index, and biomass for a variety of ecosystem types (Currit & St Clair, 2010). NDWI, a later developed vegetation index by Gao (1996), is based on the relation between the NIR region (approximately at 0.86 μm) and at the short wave infrared (SWIR) spectral region (1.24 μm):

$$NDWI = \frac{\rho NIR - \rho SWIR}{\rho NIR + \rho SWIR} \qquad (2)$$

Where *ρNIR* and *ρSWIR* are the reflectance in the NIR and SWIR spectral regions, respectively. These channels are located in the high reflectance plateau of vegetation canopies, where the absorption by vegetation liquid water near 0.86 μm is negligible and weak liquid absorption at 1.24 μm is present. As a result, NDWI is sensitive to changes in liquid water content of vegetation canopies (Gao, 1996). Note that several applications for assessing vegetation water content, substitute the 1.24 μm band with the 1.6 μm one (Ji, Zhang, Wylie, & Rover, 2011).

Combined with various biophysical variables, VIs may provide an efficient tool for monitoring regional or global-scale phenology. One example of such approach is the growing season index (GSI) model (Jolly, Nemani, & Running, 2005) that is calculated from environmental factors (minimum temperature, vapor pressure deficit, and photoperiod) and reflects canopy greenness. It is assumed that these climatic factors together account for much of the variation observed in the seasonal phenology. GSI values were then compared with phenological field observations and NDVI values and showed adequately predictions of the intra-annual dynamics of the vegetation canopy in various sites. This model showed good performance with no a priori knowledge of the local vegetation or climate (Jolly et al., 2005).

Some phenological models focused on changes in the timing and duration of phenological events as a result of specific climatic extreme events (e.g., Currit and St Clair, 2010; Nagy et al., 2013). Others (e.g., Vicente-Serrano et al., 2015; Zhou et al., 2015) focused on quantifying the effect of climate on NDVI over a restricted time scale (e.g. average seasonal NDVI, annual max NDVI), thus reflecting its influence on a certain phenological event. Only a few researches tried to model the whole yearly cycle of vegetation phenology (Jolly et al., 2005), and even less to model multiyear phenological cycles (Viskari, Hardiman, Desai, & Dietze, 2014). Statistical analysis of time series is a useful modeling approach for this type of continuous datasets (remote sensing VIs).

In the current study, the modeling approach is statistical, with integration of data and methods from remote sensing models. Remote sensing VIs were used as a proxy to the phenology of trees, while the following potential climatic constraints to plant growth, i.e., temperature, radiation, and water availability in the form of precipitation (denoted hereafter as climatic variables) were used as predictors. These variables are the main growth-limiting factors that interact to impose complex and varying limitations on vegetation activity in different parts of the world (Kramer et al., 2000; Li et al., 2013; Nemani et al., 2003). It is important to note that this analysis is primarily concerned with climate factors influencing plant phenology, and aims to produce a model that is simple to implement. Therefore, other additional important factors that can also alter tree growth - such as soil texture (Zhao et al., 2013), nutrients (Nemani et al., 2003), CO_2 concentrations (Cleland et al., 2006), and pest phenology (Zhao et al., 2013) were not taken into account in the analysis. This model strives to explain and predict continuous multi-year phenological cycles, rather than specific phenological events.

1.3 Phenological monitoring using proximal remote sensing techniques

Although satellite imagery data can be useful for phenological monitoring (Connor, Dwyer, & Cawkwell, 2008), it also has major limitations of spatial and temporal resolution. On the other hand, traditional ground-based phenological measurements place their own challenges, as they require proficient manpower, they are labor intensive, and are difficult to extrapolate over large scales (Hufkens et al., 2012). Recently, alongside the use of data retrieved from sensors abroad satellites for detecting leaf phenology, near-surface remote sensing using conventional or networked red–green–blue (RGB) cameras has been applied in various regions (Crimmins & Crimmins, 2008; Graham, Riordan, Yuen, Estrin, & Rundel, 2010; Richardson et al., 2007; Richardson, Braswell, Hollinger, Jenkins, & Ollinger, 2009; Sonnentag et al., 2012). These near surface remote sensing methods are becoming widely used in the last decade as they overcome on some of the limitations of the common used methods.

Near-surface remote sensing was used to study phenology of different vegetation types, starting form grasslands (Julitta et al., 2014) up to dense forested plots (Sonnentag et al., 2012). Phenology was monitored using relatively simple vegetation indices that are based on the relations between the normalized brightness of the green band and the normalized brightness of red and blue bands (Julitta et al., 2014). These researches demonstrated that using near-surface remote sensing techniques can accomplish large-scale and high resolution phenology monitoring (Graham et al., 2010). Moreover, as recent studies have shown an agreement between phenological time series and remote sensing matrices (Hufkens et al., 2012), data obtained through near surface sensors can potentially be up scaled (calibrated to remote sensors) to be used for large scale analyses.

In spite of the extent use of simple RGB cameras (Garonna et al., 2014; Hufkens et al., 2012; Julitta et al., 2014; Richardson et al., 2007, 2009), to the best of the author knowledge, none of the above-mentioned studies have used VIS-NIR multispectral cameras for phenological monitoring. The information that lies within the NIR spectral range is valuable for the study of vegetation phenology, as changes associated with phenological events are expressed in it. For example, internal structural changes due to leaf senescence have a clear effect on the reflectance in the NIR region. Near-infrared reflectance (700-1300 nm) initially rises as the number of scattering interfaces increases as cells split and cell contents shrink away from cell walls, and eventually decreases in accordance with further mesophyll breakdown (Castro & Sanchez-Azofeifa, 2008). The combination of information about the structural changes and pigment content can be expressed in vegetation indices such as NDVI (Tucker, 1979), and may serve as a more advanced phenology index as compared with traditional RGB based indices. Nonetheless, the determination of phenological stages is species-specific and, therefore, other biological (physiological or anatomical) factors may be required to spectrally-account for cyclic changes in the plant.

Alongside the advantages that lie in using higher amount of spectral bands, there is also a potential improvement in the ability to use reflectance data. Such data is normalized according to the prevailing illumination conditions in each day, thus minimizing the effects of diurnal, seasonal and weather-related changes in scene illumination. Improving the quality of the available data will allow acquiring data with higher temporal resolution. Evaluating the performance of multispectral camera for phenological monitoring might offer a new methodological direction for long-term phenological studies.

1.4 Research objectives

The aim of this research is twofold: (1) to study the phenological behavior of four forests located along the climatic gradient in Israel, as a response to potential climatic constraints to plant growth during the last 15 years (2000-2014); and (2) to explore the performance of a VIS-NIR multispectral camera in assessing a year-round phenological cycle. Specific objectives are as follows:

1. To examine which vegetation index (NDVI or NDWI) is more suitable for phenological modeling.

2. To create a time series prediction model that quantifies the effect of potential climatic constraints to plant growth (e.g., precipitation, temperature, radiation) on vegetation indices.

3. To monitor phenological events related to the vegetative growth. Note that this research did not focus on monitoring blooming and fruiting events, due to the difficulty to distinguish between these elements and the rest of the canopy.

1.5 Research Hypotheses

1. VIs are expected to have higher correlations with precipitation anomaly than with temperature and radiation anomalies, as Israel is located in a water limited area. The relative importance of precipitation anomaly is expected to decrease with the climatic gradient, due to the decrease in the aridity towards north.

2. It is expected that NDVI and NDWI will have different relations with the climatic variables, as NDWI is more related to changes in canopy water content while NDVI is more related to changes in photosynthetic activity.
3. Correlation between phenology and climatic variables can be used for the prediction of future phenological cycles.
4. NDVI time series retrieved from a multi-spectral camera is feasible for phenological monitoring, as they reflect changes in parameters associated with the vegetative phenological stage (LAI, productivity and biomass).

2. Methodology

2.1 Study area

Phenological models were created for four sites (from south to north) that are located in southern Judea Mountains (Yatir), Jerusalem Corridor, the Carmel Ridge, and the Upper Galilee. The climatic gradient (as defined by the aridity index) extends from arid to dry sub-humid (Fig**. 1**) where the annual rainfall average ranging from 275 to 850 mm and the potential evaporation from 1400 to 1600 mm. These forests differ in the composition of the natural tree and shrub species and in the planted trees as well (Table 1). The climate over the entire study area is characterized by winter rains occurring mainly during November through March, and a relatively long, dry, hot summer (Osem et al., 2009).

Beside the above-mentioned forests, a separate part of the research was conducted at Ramat HaNadiv Park. The park that is located at the southern end of Mount Carmel (32°33'25.62"N, 34°56'21.46"E) was chosen as a site for operating the multispectral camera. The camera observed the north-facing slope that is mainly dominated by three evergreen sclerophyll trees: Mock privet (*Phillyrea latifolia*), Green olive (*Olea europaea*), Oak (*Quercus calliprinos*), and Mastic shrubs (*Pistacia lentiscus*). These evergreen tree and shrub species are typical to Mediterranean ecosystems with phenological patterns that are characterized generally by short intensive vegetative growth and blooming in the spring. The vegetative stage is timed with maximal water availability and temperature rise (Pollak, Swartz Tzahor, & Perevolotsky, 2001). Evergreen species often express only small seasonal fluctuations in LAI with a full canopy retained throughout the year, due to their ability to access deep soil stores of water and ground water (Ma et al., 2013) resulting from rapid development of deep roots (Hasselquist, Allen, & Santiago, 2010).

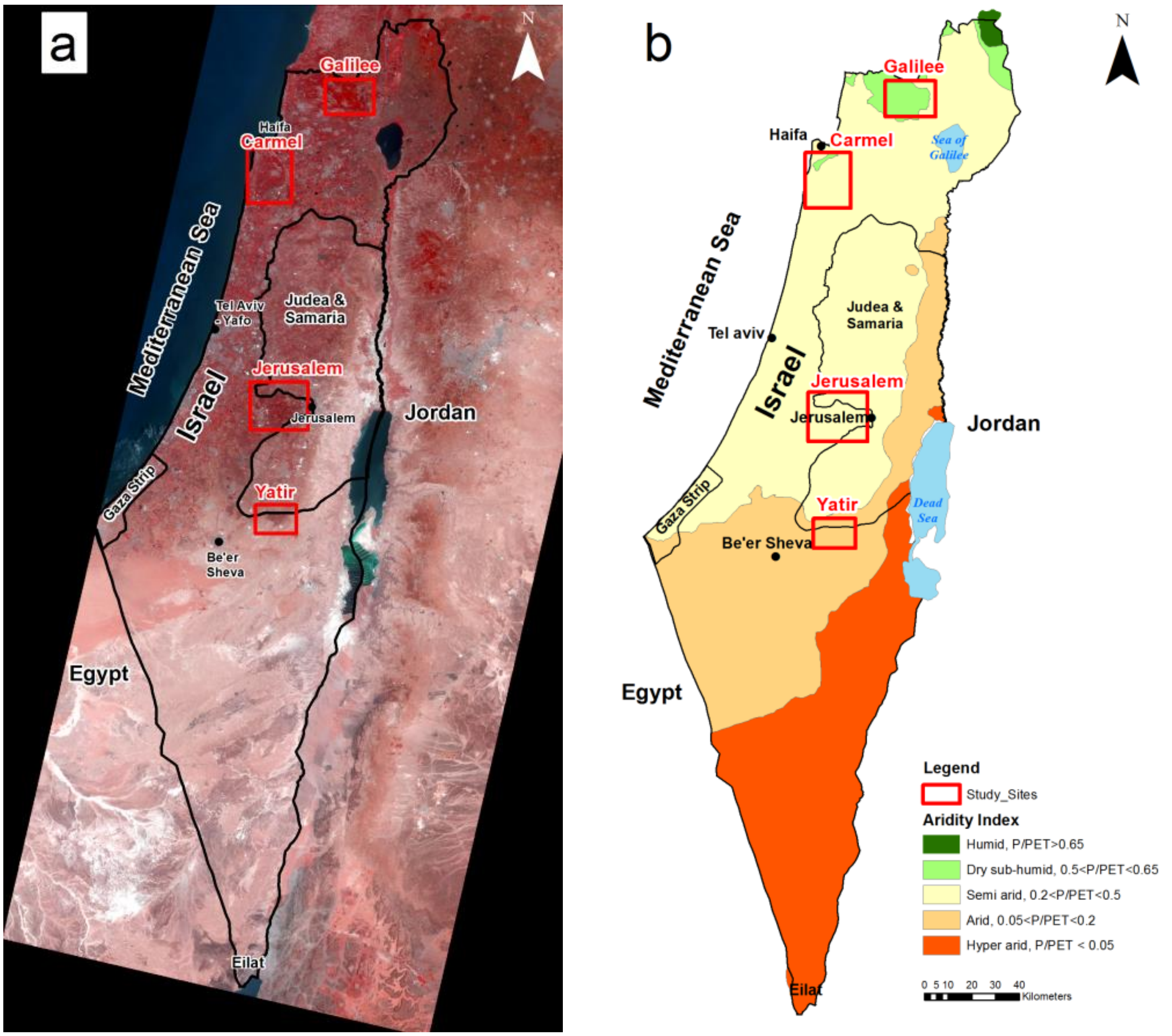

Fig. 1. Study sites maps: (a) Satellite image of Israel (false color composite of Landsat 8 images) and the four forest study sites; (b) Study sites locations along climate zones in Israel. Climatic zones are defined by the aridity index (Safriel, 2014).

Table 1. Characterization of four study sites

	Study sites				Reference
	Yatir	Jerusalem Corridor	Carmel	Galilee	
Coordinates (Lat/Long)	31°20'20.90"N 35° 3'29.77"E	31°45'34.88"N 35° 3'55.15"E	32°39'51.37"N 35°2'0.67"E	32°59'29.93"N 35°23'22.30"E	
Climatic zone	arid	semi-arid	semi-arid to dry sub-humid	dry sub-humid	(Safriel, 2014)
Annual Rainfall (mm)	275	500-700	550-750	750-900	(Shahar, 1995)
Potential evaporation (mm)	1600	~1600	~1400	~1400	
Forest Characterization	Planted trees	Planted & natural trees	Planted & natural trees	Planted & natural trees	(Y. Osem, Pers. Commun.)
Vegetation	Planted trees: mainly with *Pinus halepensis.*	Coniferous tree species: mainly *P. halepensis*, *Pinus brutia*, and *Cupressus semperviren* but also *Pinus pinea* and *Pinus canariensis* Shrubs mainly *Pistacia lentiscus* and dwarf shrubs *Sarcopoterium spinosum*	Natural woodlands and shrublands: dominated by *P. halepensis*, *Q. calliprinos*, *Pistacia* (trees), and *Pistacia lentiscus* (shrubs)	Natural woodland: dominated by *Q. calliprinos*, *Laurus nobilis* (in the more humid areas) and *Quercus boissieri* (in areas exceeding 600 m ASL)	
	Natural vegetation: dwarf *shrubland* dominated mainly by *Sarcopoterium spinosum*	Broadleaved species: *Eucalyptus camaldulensis*, *Ceratonia siliqua* Natural woodland trees: mainly *Quercus calliprinos*	Planted trees: *P. halepensis*, *P. brutia* and *C. sempervirens* but also *P. pinea* and *P. canariensis.*	Planted coniferous trees: similar to the ones described for the Carmel and Jerusalem mountains.	

2.2 Satellite data

NDVI and NDWI data for 2000-2014 (16-day composite, 250 m spatial resolution) were downloaded from a global time-series database of the Global Agricultural Monitoring (GLAM) project (http://pekko.geog.umd.edu/usda/test/) (Becker-Reshef et al., 2010). These data were derived from the MODIS instrument onboard the Terra spacecraft. The NDVI, calculated from MODIS bands 1 (620–670 nm) and 2 (841–876 nm), was used as a measure of forest performance, reflecting green biomass quantity, and state. NDWI calculated from MODIS bands 2 (841-876 nm) and 6 (1628-1652 nm), provided a measure of vegetation water content. Both indices provide measures to the phenological state of forests, however since the red band is sensitive to leaf chlorophyll concentration, the NIR band to the leaf cell structure, and the SWIR one to the leave water content, the two indices should be considered as independent ones (Gao, 1996). The indices were averaged for the polygon that delineated the forest *per se* excluding non-forested areas (e.g. settlements, clearings, etc.).

2.3 Meteorological data

Daily precipitation, air temperature (minimum, maximum and average), and global radiation data were retrieved from the Israeli Metrological Service web sites (https://data.gov.il/ims) for each forest. Temperature and radiation data were downloaded from the closest monitoring stations available. In order to better represent the amount of precipitation over the forest area, precipitation data from several stations were interpolated for each forest area using a Thiessen method (Ohana-Levi, Karnieli, Egozi, Givati, & Peeters, 2015).

2.4 Statistical model

The entire dataset (15 years, 2000-2014) was divided into a training period (the first 200 observations) and a validation period (the following 133 observations). The training period was used to evaluate the existing relations between VIs and the potential climatic constraints to plant growth (i.e., precipitation, temperature, and radiation), while the validation period was used to evaluate the predictive skills of the model (Fig. 2). In order to study the relations between the climatic variables and the spectral VIs, a time series analysis was conducted. It was assumed that phenological events are a result of accumulated effect of climatic variables, and can occur after a certain time-lag. Accordingly, the response of VIs to different accumulation periods and time-lags of climatic variables was examined. This was carried out by creating a matrix of cross correlation results between the vegetation index and prior moving average (PMA) precipitation/temperature/radiation for different periods (up to three years) and different time-lags (up to three years), with time steps of 16 days. For each climatic variable, the PMA and lag components that created the highest cross correlation with the VIs were chosen for further analysis.

The cycle components of VIs and climatic variables were derived using Fast Fourier Transform (FFT) that decomposes the time series into simpler periodic signals in the frequency domain (Lhermitte et al., 2008). By discarding higher order harmonics while retaining the first-order and second-order harmonics, it is possible to retrieve lower noise signals that characterize the basic temporal behavior of the vegetated surface (Beurs Kirsten M.de & Henebry, 2010). This technique was shown to be particularly useful for NDVI time series analysis for describing and quantifying fundamental temporal characteristics (Lhermitte et al., 2008).

The FFT analysis was implemented on VIs and the climatic variables. This part of the analysis was applied on the first 200 observations that served as a training period. The FFT of each series was derived and the frequencies were ranked by their amplitudes (form large to small). A new time series was obtained by: (1) keeping the first n frequencies (those with the largest amplitudes) while setting the amplitude of all other frequencies to zero; and (2) inverting this modified FFT series. The cross-correlation between the new time series (i.e., the one obtained from the VI series and the one from the climatic variable series) was calculated. The number n was set by the requirement that the cross-correlation will be maximal. The time series with maximal cross-correlation were defined as the trends of the series. Identifying these trends/cycles enabled us to examine the influence of climatic variables anomaly on VI anomalies. Anomalies were calculated as the differences between the measured data and the trends. In addition, the series were also examined for temporal trends that are independent of the cross-correlation with the other variables. The data were averaged annually and the effect of time (t, t^2, t^3) was evaluated. The final models were composed from the cycle component and the anomalies of the climatic variables that had significant effect on the VIs.

Predicted time series (last 133 observations) was created using the coefficients and cycles that were retrieved from the analysis of the training period. Anomaly of climatic variables was calculated as the shift of the measured climatic variables from the cycles that were retrieved from the training period. Prediction abilities were evaluated by two measures:

(1) Normalized Root Mean Square Error (NRMSE). This method compares two datasets and provides a measure to the difference between the predicted time series by the model and the actual observed time series:

$$NRMSE = \sqrt{\frac{1}{n}\sum_{t=1}^{n} \frac{(P_t - O_t)^2}{\frac{1}{2}(|O_t| + |P_t|)}} \tag{3}$$

Where P_t is the predicted time series, O_t is the observed time series, and n is the number of observations.

(2) Adjusted R^2 results from the linear regression between the observed VI time series (in the validation period) and the variables that are used for the prediction process, namely, the cycle component that was calculated from the first 200 observations and the anomaly of observed climatic variables from the calculated cycles of these variables (on the basis of the first 200 observations). This analysis measures the fit of the observed data in the validation period to the cycles that were retrieved from the training period and the anomalies of the observed climatic variables.

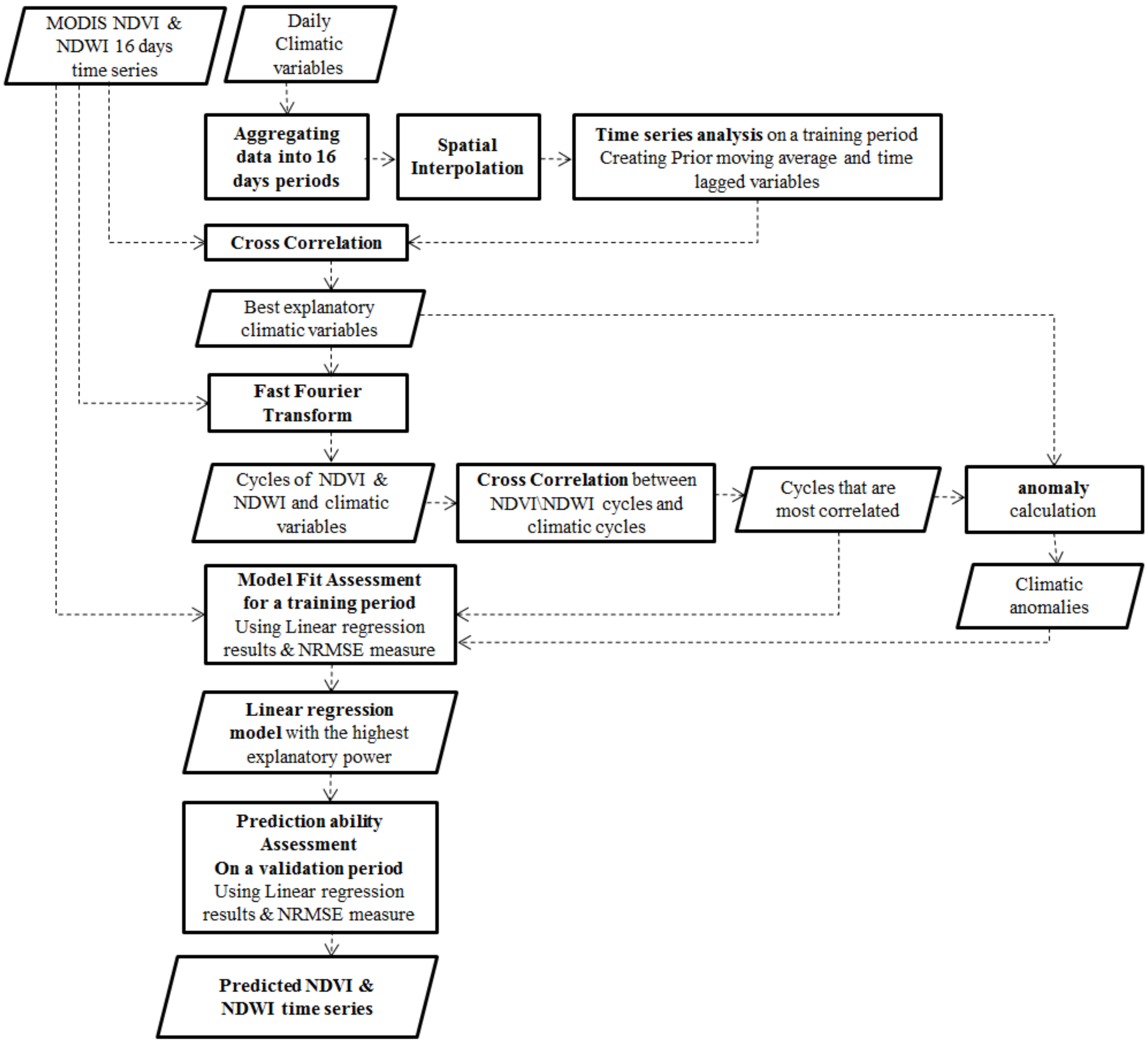

Fig. 2. Flowchart for time series analysis

2.5 Year round phenological monitoring

In order to explore the performance of the multispectral camera and assess a year-around phenological cycle, a Mini MCA camera (Tetracam, Inc. Chatsworth, USA) was installed on a monitoring tower located on the north facing slope (Fig. 3). The camera was equipped with five spectral bands that were centered along the green (550 nm), red (670 nm), red edge (740 nm, 780 nm), and NIR (860 nm) spectral regions, with band width of 10 nm. An additional sixth band was converted into the incident light sensor (ILS) that gathers the down-welling radiation, so that radiation flux units could be converted into normalized reflectance values. It was located in the upper part of the box looking upwards to the sky. The camera was connected to computer with internet connection (Fig. 3), which allowed transferring the data daily to the lab. Since the camera was observing a slope, pixel size ranged from 7-16 cm, depending on the distance from the camera. Images were taken on an hourly-basis during solar midday, from between 10:00 and 13:00, using the automatic exposure mode.

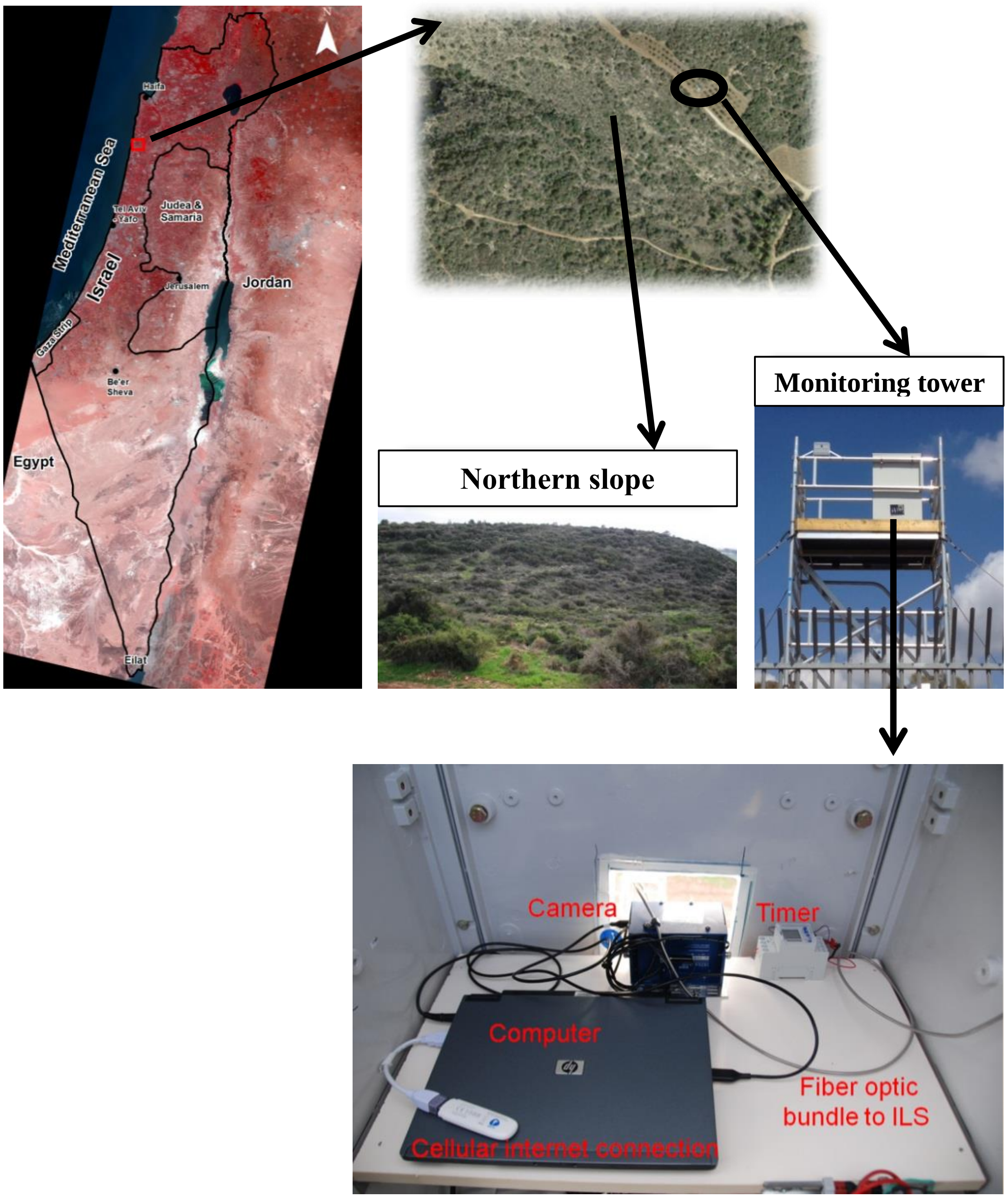

Fig. 3. Experimental setting in Ramat HaNadiv Park

Image pre-processing procedure (Fig. 4) included the following processing steps. Firstly, all images were visually inspected in order to exclude those that were too dark and/or clouded. For each suitable day, three images were selected, in order to minimize the effect of different solar inclination. All images were converted from RAW format into TIFF formats and into reflectance values using PixelWrench software (Tetracam, Inc. Chatsworth, USA). All necessary geometric corrections were done using ERDAS Imagine software (ERDAS, Norcross, USA 2015). The statistical analysis stage included daily average calculation and creating monthly NDVI time series. Pixels with NDVI values of 1 were masked, as they represent pixels with saturation problem. Eventually, statistical measures of NDVI were calculated for each monitored tree, in a monthly time-scale. Trees were marked by polygons which included the sun exposed parts only.

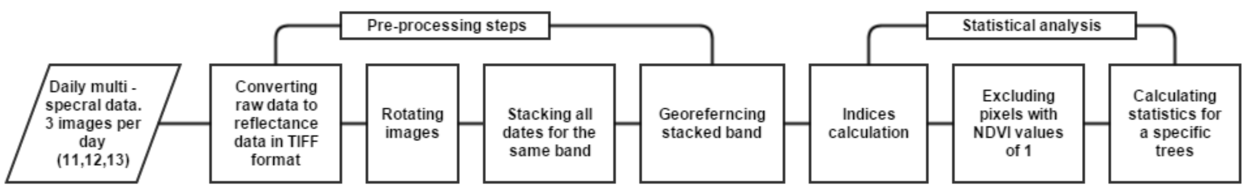

Fig. 4. Flowchart of the image processing and data retrieval

2.6 Physiological measurements

To support the observed phenological processes, physiological measurements were conducted during representative dates in each season, on the leaves of 24 selected trees (six individuals of each of the four dominant species; Fig. 5). In this framework leaf water potential (Ψl; reflecting water availability), stomata conductance (gs; reflecting plants' main response to water limitation, through changes in stomata aperture), and chlorophyll concentration (Chl; reflecting vegetation greenness and the ability to perform photosynthesis) values were measured. All three variables are correlated and complement each other (Williams & Araujo, 2002), and have been shown to be relevant for phenological studies (Eamus, 1999).

Values of leaf water potential were collected with a Scholander pressure chamber (PMS Instrument Co., Corvallis, Oregon, USA) from three brunches per tree. Youngest fully-matured samples were collected twice a day; once at pre-dawn (about an hour before sunrise) in order to account for soil water availability, and once at solar noon in order to assess the water balance during maximum stress and to coincide with the spectral observations. Practically, excised brunches were immediately stored in cooled, sealed plastic bags until all samples were acquired (around half an hour). In accordance with the Ψl observations, stomata conductance (gs) values were also measured twice - once during the morning (between 8:00-9:30) and at midday - using a leaf porometer (Decagon Devices, Inc., Washington, USA). Four sun-exposed, youngest fully-matured leaves were selected from each tree.

For Chl measurements one representative brunch was selected from each tree and stored in ice until reaching to the laboratory. Analysis was conducted on the next day according to the following steps: (1) 3-4 representative leaves were chosen from each tree; (2) 20 mg sample was weighted from each leaf and stored in a 2 ml Eppendorf tube; (3) The tubes with the samples were frizzed using liquid nitrogen and crushed by shaking the tubes with added metal balls in a shaker for 5 minutes; (4) 1.5 ml of 95% Ethanol were added to the tubes, and shacked for 3 to 5 hours until full extraction; (5) Tubes were centrifuged for 5 minutes in 14,000 rpm; (6) Samples were diluted by an order of 2.5, and transferred to a cuvette. 7) Absorption spectrum was measured in spectrophotometer (Evolution 220, Thermo Scientific); (8) Chlorophyll concentration was calculated by placing the absorption results in the concentration equation (Lichtenthaler & Buschmann, 2001).

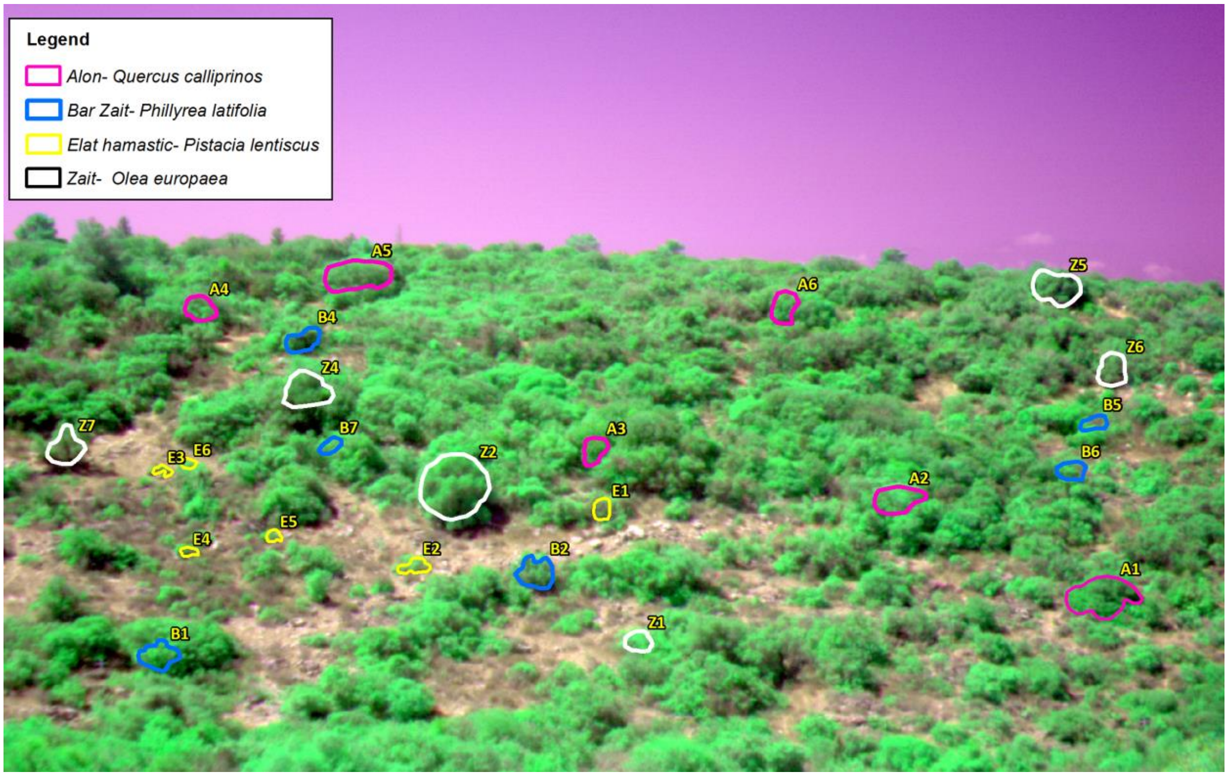

Fig. 5. Tree species distribution in Ramat HaNadiv site.

2.7 Statistical analyses and image processing

Time series analysis was performed using the R software (R Development Core Team, 2014). Spatial interpolation of precipitation data was implemented in ArcGIS 10.3 software (ESRI, Redlands, USA, 2014). All statistical analysis of the data from Ramat HaNadiv site was performed using the Statistica 12.0 software (StatSoft Inc., 2015, Tulsa, Oklahoma, USA). The significance of the differences between mean values was evaluated using one-way Analyses of Variance (ANOVA) test. Thereafter, Tukey's Honest Significance Difference (HSD) post-hoc tests were used in order to compare between specific groups. Assumptions of residuals' normality and homogeneousness of variances were checked and met using Shapiro-Wilk and Levene's tests, respectively. It should also be noted that in several cases the assumption of the homogeneousness of variances was violated, and, therefore, suitable data transformations were applied.

3. Results

3.1 Inter-site differences in VI's and climatic variables

Time series of both VI's (Fig. 6) and climatic variables (Fig. 7) present clear periodicity in the productivity of the forest as reflected by NDVI and in the leaf water content as reflected by NDWI. These time series present also distinct differences between the sites; VIs of Yatir forest are always the lowest, followed by Jerusalem, Carmel and Galilee forests, respectively (Fig. 6). Climatic variables show distinct seasonal periodicity as well, and the inter site differences are mainly reflected in the precipitation variable. Small variations in the mean temperature are observed, while the radiation is almost similar along the sites (Fig. 7).

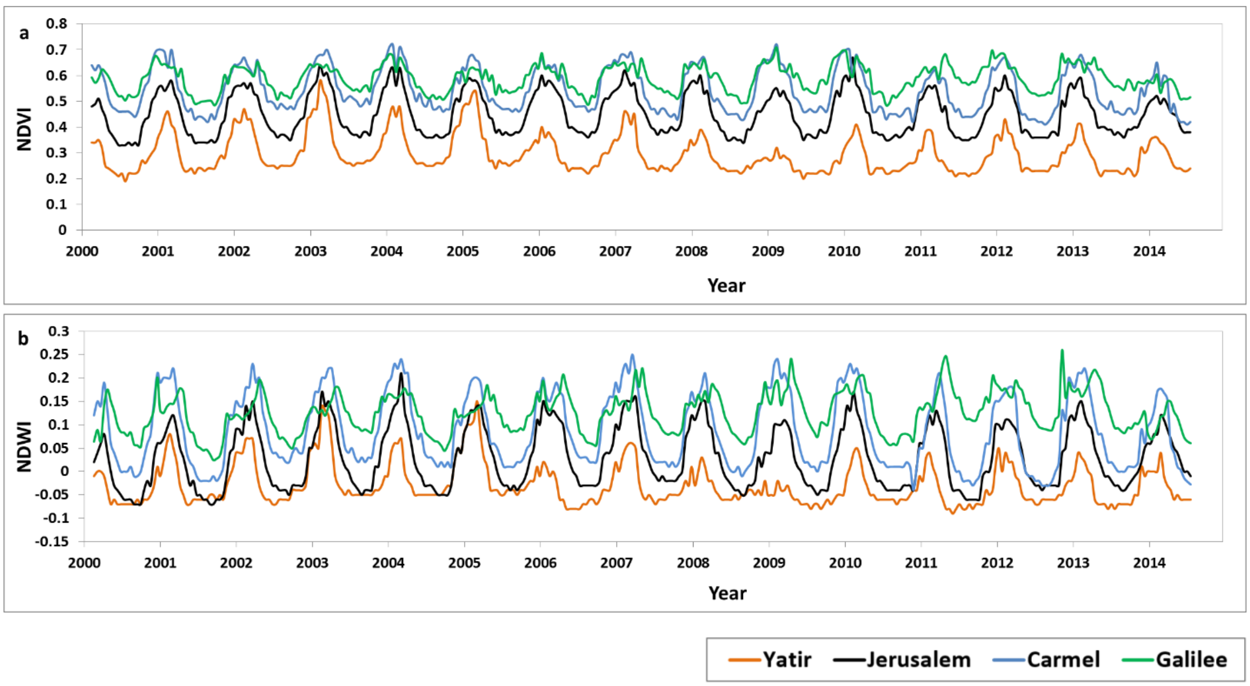

Fig. 6. VIs time series along the 15 years of study: (a) NDVI time series (b) NDWI time series.

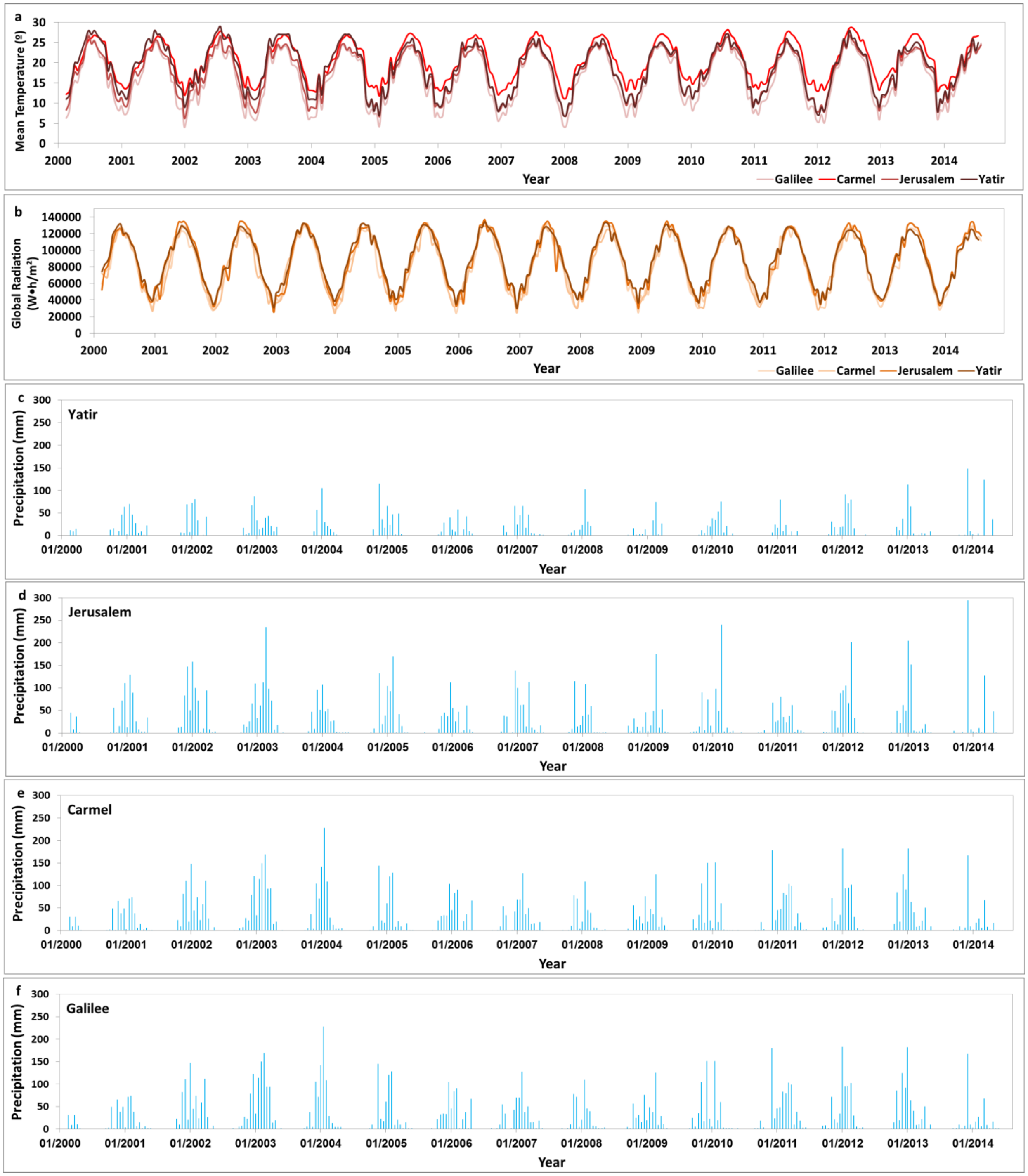

Fig. 7. Climatic variables time series along 15 years. (a) Temperature; (b) Radiation; (c-f) Precipitation.

3.2 Correlation between VIs and climatic variables

Time series analysis using linear regression models was performed on VIs and climatic variables data. In this framework, the response of VIs to different accumulation periods and time-lags of climatic variables was examined. Results from this analysis show correlations that describe climate-vegetation relations (Table 2), and are presented by the sites location from the south (Yatir) to the north (Galilee):

In Yatir site (Table 2) the highest cross-correlation was found between NDVI and accumulated precipitation in the last 80 days without time lag. The explanatory strength of the two other climatic variables was lower. The effect of radiation was found to be more pronounced with a lag of two months, while for temperature there was no pronounced effect to a time-lag. Same analysis was applied for NDWI time series, and showed similar relations with climatic variables, in terms of time-lag and PMA. However, in Yatir site the correlations of climatic variables with NDVI were higher than with NDWI.

As opposed to Yatir site, in Jerusalem site precipitation was not the main explanatory variable, as radiation and temperature produced higher adj.R^2 results with VIs (Table 2). The correlations of climatic variables with NDVI index were higher than those with NDWI. Additionally, the maximal response of NDWI to radiation and temperature occurred slightly later than with NDVI.

In the Carmel forest, the results were quite different from the two southern sites; firstly, the highest correlation with NDVI was shown with longer accumulative period of precipitation (112 days). Secondly, the correlations with the different climatic variables were rather similar, while precipitation showed the lowest explanatory power (Table 2). Thirdly, as opposed to the results from the two southern sites, the correlations with NDWI index were similar to those found with NDVI index.

Table 2. The effect of climate variables on vegetation indices. All results were highly significant (p value<0.001). cc - cross correlation results, Adj.R^2 - adjusted R^2 results, P - precipitation, T - temperature, R - radiation, PMA - prior moving average, m - month.

Yatir

	NDVI				NDWI			
Variable	PMA	Time-lag	Adj.R^2	cc	PMA	Time-lag	Adj.R^2	cc
P	2.6 m	-	0.82	0.90	2.6 m	-	0.76	0.86
R	-	2 m	0.72	-0.85	-	2 m	0.60	-0.59
T	-	0.5 m	0.65	-0.81	-	1.5 m	0.56	-0.53

Jerusalem

	NDVI				NDWI			
Variable	PMA	Time-lag	Adj.R^2	cc	PMA	Time-lag	Adj.R^2	cc
P	3.2 m	-	0.78	0.88	3.7 m	-	0.77	0.87
R	-	1.5 m	0.86	-0.93	-	2 m	0.82	-0.91
T	-	0.5 m	0.84	-0.92	-	1 m	0.80	-0.90

Carmel

	NDVI				NDWI			
Variable	PMA	Time-lag	Adj.R^2	cc	PMA	Time-lag	Adj.R^2	cc
P	3.7 m	-	0.78	0.88	4.3 m	-	0.79	0.88
R	-	2 m	0.82	-0.90	-	2.6 m	0.83	-0.91
T	-	0.5 m	0.82	-0.90	-	0.5 m	0.80	-0.90

Galilee

	NDVI				NDWI			
Variable	PMA	Time-lag	Adj.R^2	cc	PMA	Time-lag	Adj.R^2	cc
P	5.5 m	10 m	0.63	0.80	6 m	24 m	0.55	0.74
R	-	1.5 m	0.71	-0.85	-	2.5 m	0.62	-0.78
T	-	1 m	0.73	-0.83	-	2 m	0.60	-0.77

In the Galilee site, similarly to Carmel and Jerusalem sites, temperature and radiation had higher correlation with VI than precipitation, and with rather similar time lag effect. Still, it is worth noting that the influence of precipitation on VI was the lowest in this site. This site also resembled Yatir and Jerusalem sites, regarding the relations of climatic variables with VI. The correlations between NDWI and the climatic variables were lower than those of NDVI. However, the highest response of NDWI index came at a later stage, as can be seen from the higher time-lag for all the climatic variables (Table 2). The results in this site differed from those in the other sites in several aspects. Firstly, the explanatory power of all climatic variables was lower than in the other sites. Secondly, the best explanatory precipitation variable differed from those chosen in the other sites in two aspects: it was summed over a longer period (5.5 months versus 2-3 months) and there was also a pronounced time lag effect (10 months versus no significant time lag).

In all sites, the influence of PMA for temperature and radiation was examined, and shown none or only slight improvements in the correlation with VIs (data not shown); therefore, it was decided to keep these variables in their simpler version (without PMA). Additionally, no significant improvement was shown when correlating the maximal, minimal, or average temperature with VIs (data not shown) and, consequently, average temperature data was used for further analysis. All three climatic variables showed equal or higher correlation with NDVI than with NDWI (Fig. 8). Examining the correlations between NDVI and NDWI revealed that the relations between these indices are lowered (Fig. 9) with the transition from the arid southern Yatir site to the humid northern Galilee site. Another interesting finding is the relatively high range of NDVI values that exists under low NDWI values, as opposed to the convergence of NDVI values in the higher NDWI values.

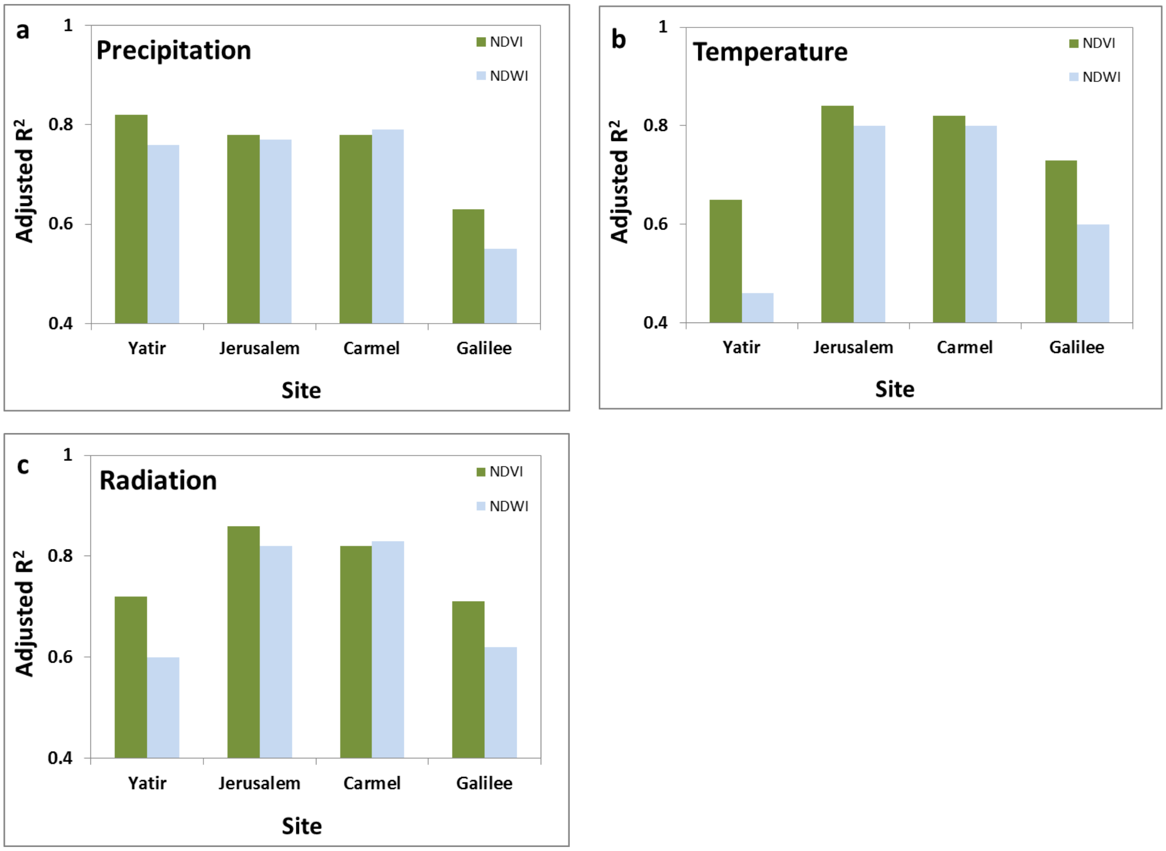

Fig. 8. Adj.R^2 results for the correlations between NDVI/NDWI and (a) precipitation; (b) temperature; and (c) radiation.

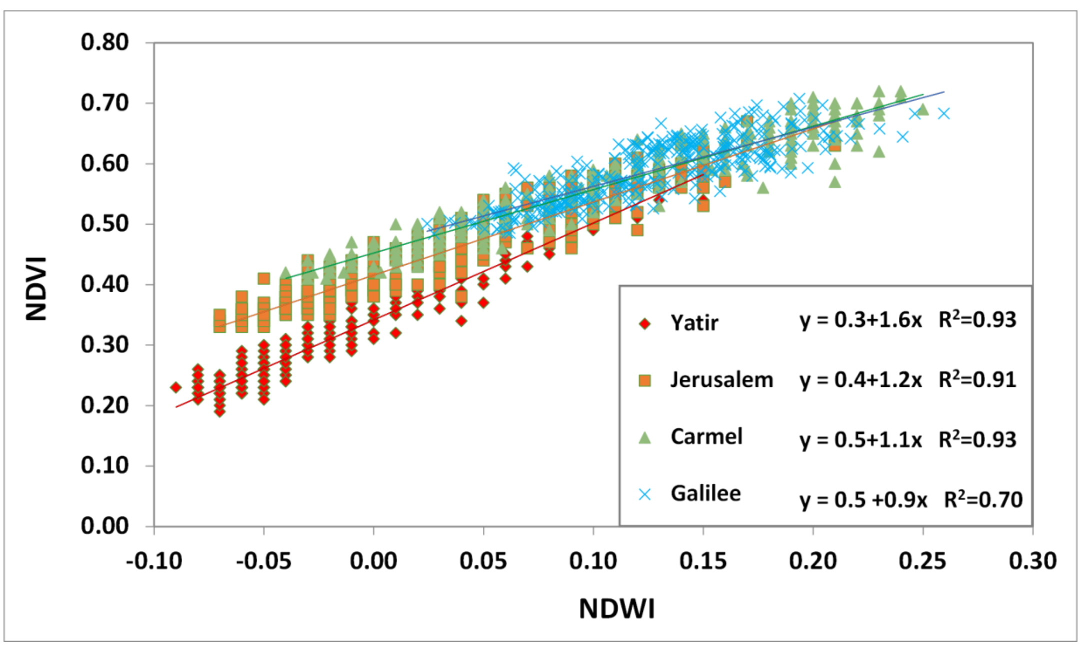

Fig. 9. Correlation between NDVI and NDWI in four forest sites.

3.3 Decomposing model

Both VIs were found to be highly correlated with all climatic variables (Table 2), hence the cycle component for VIs was chosen on the basis of the cross-correlation between the cycles of the two time series (one obtained from the VIs series and one from the climatic variable series). In Yatir site, the highest cross correlation (cc = 0.98) was found between VI's cycle and precipitation cycle, which was composed from two dominant frequencies. As for the two other variables, strong negative cross correlation (cc = -0.99) was found for cycle with a single dominant frequency. In both cases, the period was around one year. It was found that the cycle component that exists in both dependent and explanatory variables, explained the majority of variance existing in NDVI (adj.R^2 = 0.67) and in NDWI (adj.R^2 = 0.50). Taking into account the anomaly in precipitation improved the adj.R^2 of NDVI model to 0.84 and that of NDWI to 0.78, while adding anomalies of temperature and radiation, did not improve model's performance. Exploring the existence of trend using polynomial time components (t, t^2, t^3) in a yearly based NDVI and NDWI time series, showed that there was no significant time trend (Fig. 19 in appendices). The general models are described in equations 4.1 and 4.2.

In Jerusalem site, cycle component retrieval from the highest cross correlation with the cycles of climatic variables showed that there is one main yearly cycle. Similarly to Yatir site, the cycle component explained much of the variance (adj.R^2 = 0.71) in NDVI and in NDWI (adj.R^2 = 0.69). Anomalies of all three variables had significant effect in NDVI's explanatory variable; however for NDWI's model only precipitation and temperature had significant effect. No significant yearly time trend was found (Fig. 19 in appendices). The general models are described in equations 5.1 and 5.2.

In Carmel site, the cycle of all climatic variables showed the highest cross correlation with the cycle of one dominant frequency retrieved from NDVI and NDWI time series. The period of this cycle is one year. In this site the cycle component explained much of the variance (adj.R^2 = 0.67) in NDVI time series and in NDWI time series (adj.R^2 = 0.50) as well. After including precipitation and temperature anomalies, the effect of the anomaly of radiation was insignificant, and therefore, it was not included in the final model. Exploring the existence of trend using polynomial components (t, t^2, t^3) in both VIs showed that there was no significant trend (Fig. 19 in appendices). The general models are described in equations 6.1 and 6.2.

In Galilee site, cycle component extraction from maximal cross correlation (cc = 0.96 for NDVI and cc = 0.99 for NDWI) with precipitation variable showed one dominant cycle with a period time of one year. Slightly higher cross correlation (cc = -0.98 for NDVI and cc = -0.99 for NDWI) was found with the cycle of temperature and radiation. This cycle was constructed from two main frequencies that both fluctuate around one year. Similarly to other sites, the cycle component explained much of the variance in NDVI (adj.R^2 = 0.64) and in NDWI (adj.R^2 = 0.48). Differently from the other three southern sites, radiation and temperature anomalies produced the highest explanatory model for NDVI (adj.R^2 = 0.76), while adding precipitation anomaly was insignificant to the performance of the model. No significant yearly time trend was found for NDVI time series (Fig. 19 in appendices). For NDWI, best explanatory model (adj.R^2 = 0.63) was achieved by adding precipitation and radiation anomalies. Differently from all other sites, there was a significant positive trend in the yearly average NDWI values (Fig. 19 in appendices). The general models for this site are described in equations 7.1 and 7.2.

$$\boldsymbol{NDVI_{t\,(Yatir)}} = C_t + f(P_{anoamly}(t)) + \mathcal{E}_t,\ t = 1, \dots, n. \qquad (4.1)$$

$$\boldsymbol{NDWI_{t\,(Yatir)}} = C_t + f(P_{anoamly}(t)) + \mathcal{E}_t,\ t = 1, \dots, n. \qquad (4.2)$$

$$\boldsymbol{NDVI_{t\,(Jerusalem)}} = C_t + f(P_{anoamly}(t)) + f(R_{anoamly}(t)) + f(T_{anoamly}(t)) + \mathcal{E}_t,\ t = 1, \dots, n. \ (5.1)$$

$$\boldsymbol{NDWI_{t\,(Jerusalem)}} = C_t + f(P_{anoamly}(t)) + f(T_{anoamly}(t)) + \mathcal{E}_t\ ,\ t = 1, \dots, n. \ (5.2)$$

$$\boldsymbol{NDVI_{t\,(Carmel)}} = C_t + f(P_{anoamly}(t)) + f(T_{anoamly}(t)) + \mathcal{E}_t\ ,\ t = 1, \dots, n. \qquad (6.1)$$

$$\boldsymbol{NDWI_{t\,(Carmel)}} = C_t + f(P_{anoamly}(t)) + f(T_{anoamly}(t)) + \mathcal{E}_t\ ,\ t = 1, \dots, n. \qquad (6.2)$$

$$\boldsymbol{NDVI_{t\,(Galilee)}} = C_t + f(R_{anoamly}(t)) + f(T_{anoamly}(t)) + \mathcal{E}_t, \;\; t = 1, \dots, n. \quad (7.1)$$

$$\boldsymbol{NDWI_{t\,(Galilee)}} = C_t + f(P_{anoamly}(t)) + f(T_{anoamly}(t)) + T_t + \mathcal{E}_t, \;\; t = 1, \dots, n. \quad (7.2)$$

Where $NDVI_t$ and $NDWI_t$ are the observed data at time t, C_t is the cycle component, T_t is the yearly time trend, $P_{anomaly}$, $T_{anomaly}$, and $R_{anomaly}$ are the shifts of precipitation, temperature, and radiation from their cycle, and $\mathcal{E}_t$ is the remainder component.

3.4 Validation period

In all sites the correlations between VIs and the climatic variables in the training period were higher than those in the validation period (Table 3). The lowest prediction ability, expressed by the lowest adj.R^2 and the highest NRMSE results, was shown in the northern Galilee site and the southern Yatir site (Table 3). In Yatir site, prediction overestimated VIs as comparison to actual measurements (Fig. 10 & 11.a). In Galilee site, the observed data was noisy relatively to the other sites (Fig. 10 & 11.d). However, along all of the period and in all sites, prediction was within the internal spatial standard deviation of the data.

Table 3. Evaluation parameters for model's performance for VIs time series. NRMSE- normalized root mean square error, Adj.R^2- adjusted R^2. All models were highly significant (p value<0.001).

NDVI

	Yatir		Jerusalem		Carmel		Galilee	
	Adj.R^2	NRMSE	Adj.R^2	NRMSE	Adj.R^2	NRMSE	Adj.R^2	NRMSE
Training	0.84	0.06	0.81	0.05	0.87	0.04	0.76	0.03
Validation	0.66	0.09	0.78	0.06	0.78	0.06	0.54	0.05

NDWI

	Yatir		Jerusalem		Carmel		Galilee	
	Adj.R^2	NRMSE	Adj.R^2	NRMSE	Adj.R^2	NRMSE	Adj.R^2	NRMSE
Training	0.78	0.12	0.82	0.13	0.84	0.10	0.67	0.08
Validation	0.73	0. 15	0.79	0.18	0.79	0.14	0.42	0.11

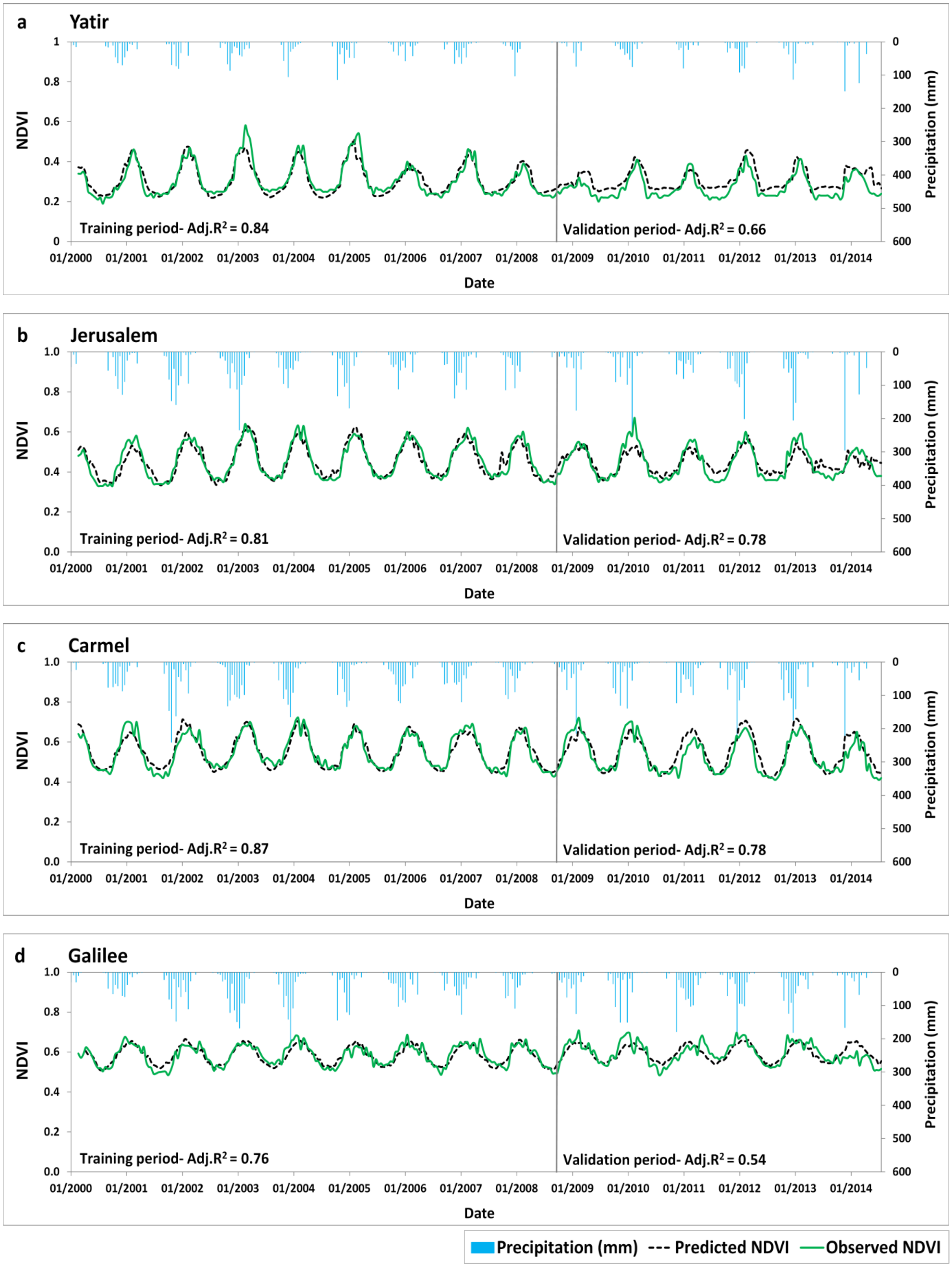

Fig. 10. Time series analysis results for NDVI time series for the four sites.

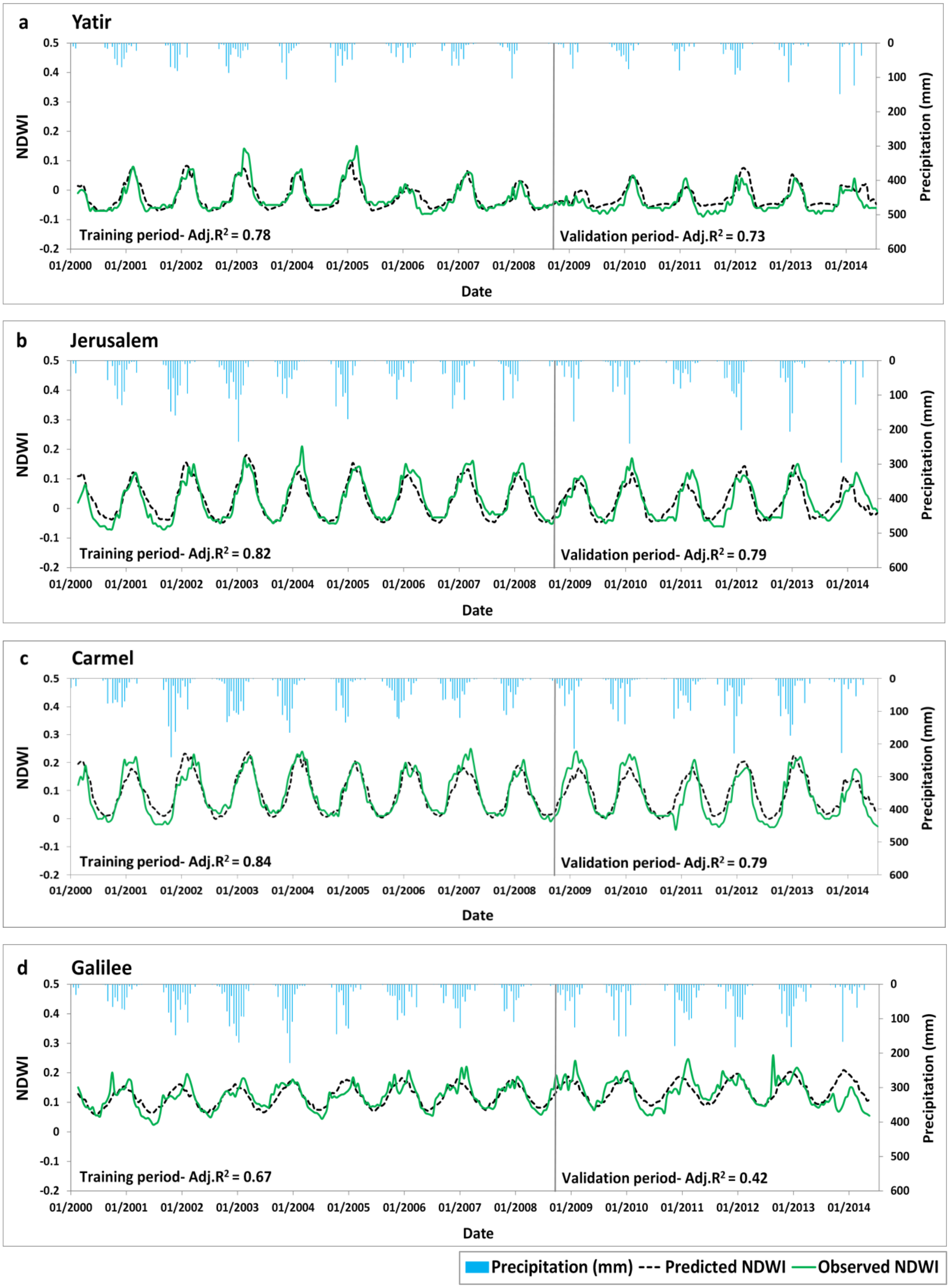

Fig. 11. Time series analysis results for NDWI time series for the four sites.

3.5 Phenological monitoring in Ramat HaNadiv site

NDVI changes were evident both for the entire plot scale (Fig. 12.a) and for individual species (Fig. 12. b-e). In the plot scale, a response in NDVI values to precipitation regime was observed, as NDVI values dropped to a minimum in October, after a long dry spell and a recovery trend identified with the renewal of rain season (Fig. 12.a). The phenological cycle of the three tree species was alike, with maximal NDVI values in spring and summer, minimal NDVI values occurring in the winter time, and increasing NDVI values towards spring months (Fig. 12.a-b). *P. lentiscus* shrubs differed in their phenological cycles from the three other species; minimal NDVI values were observed already in the summer months and started to rise from September (Fig. 12.e). Although the differences between the months were not significant (Fig. 12), there were some significant differences between the months that represent the peak of seasons, especially between the peak of the first spring season (April 2014) and the rest of the seasons (Fig. 13). In all species the standard deviation was the highest in the winter months, probably reflecting different timing of start of vegetative growth.

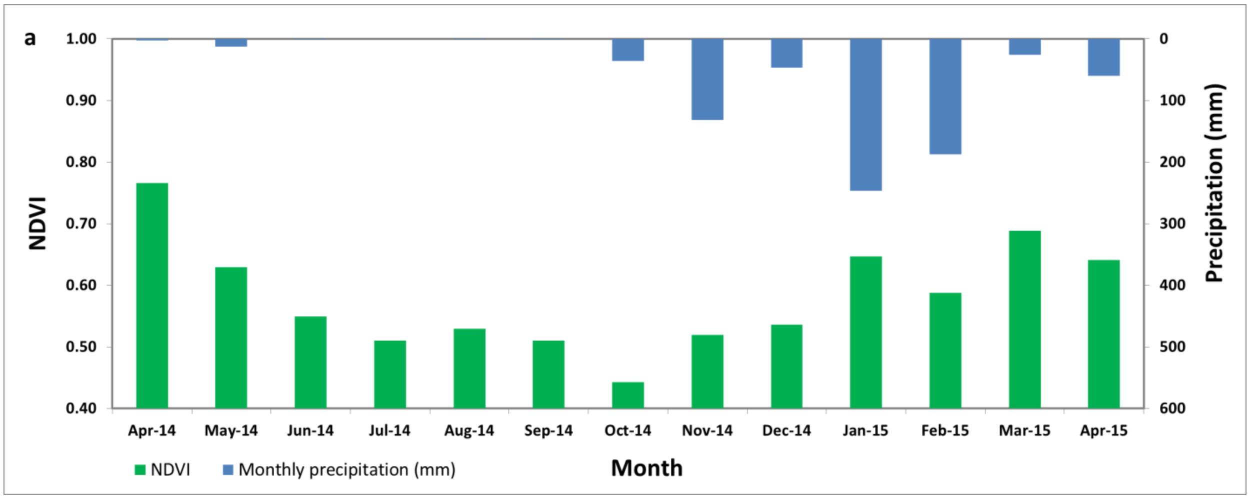

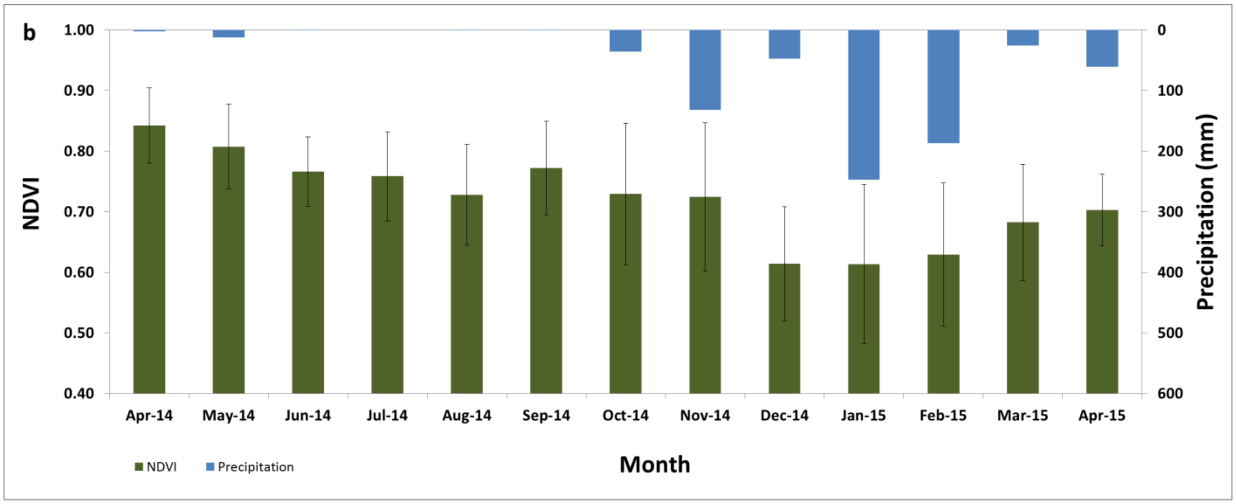
b
NDVI
Precipitation (mm)
Apr-14
May-14
Jun-14
Jul-14
Aug-14
Sep-14
Oct-14
Nov-14
Dec-14
Jan-15
Feb-15
Mar-15
Apr-15
NDVI
Precipitation
Month

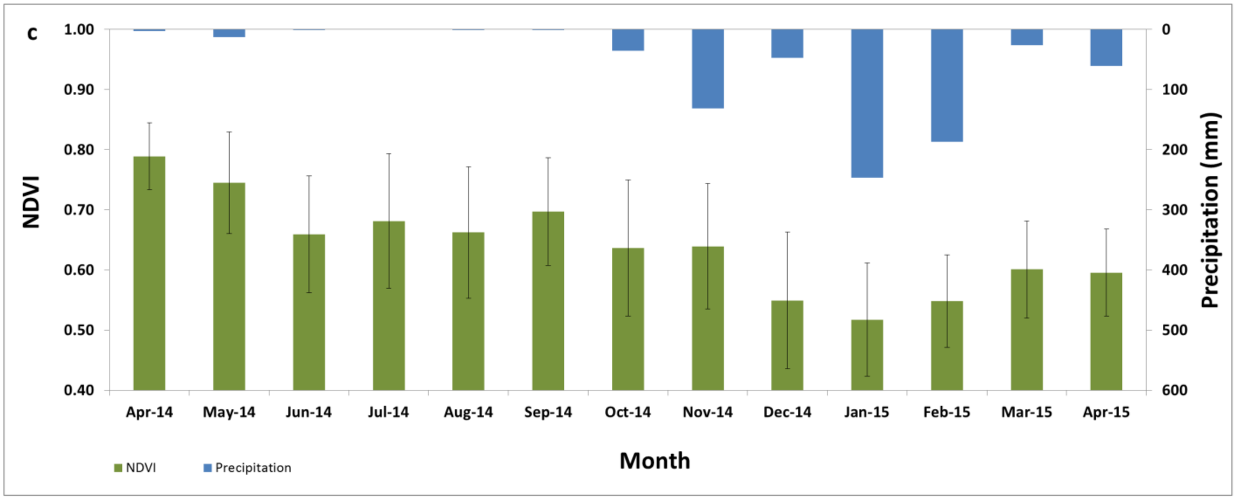
c
NDVI
Precipitation (mm)
Apr-14
May-14
Jun-14
Jul-14
Aug-14
Sep-14
Oct-14
Nov-14
Dec-14
Jan-15
Feb-15
Mar-15
Apr-15
NDVI
Precipitation
Month

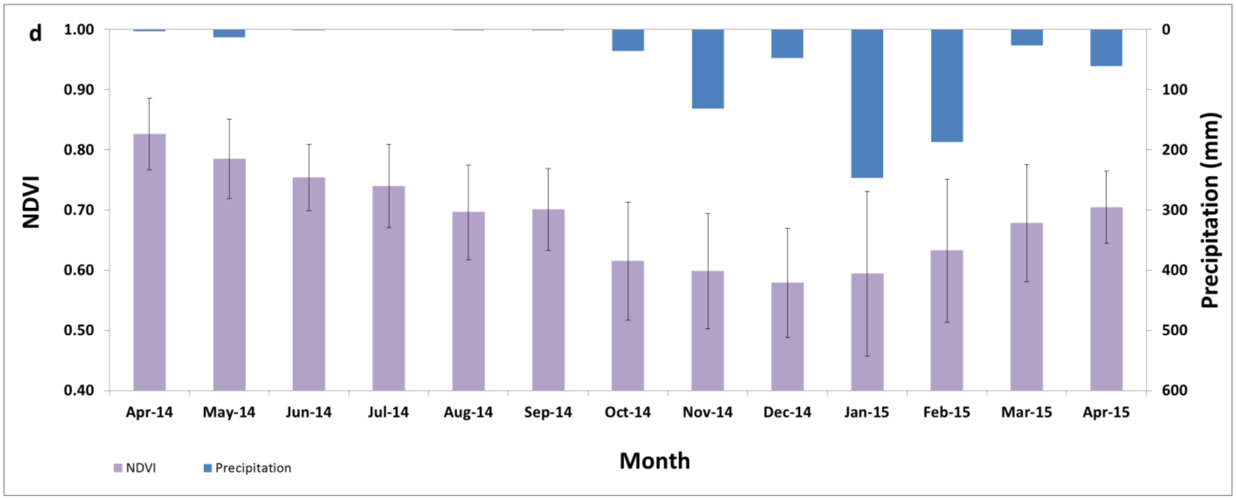
d
NDVI
Precipitation (mm)
Apr-14
May-14
Jun-14
Jul-14
Aug-14
Sep-14
Oct-14
Nov-14
Dec-14
Jan-15
Feb-15
Mar-15
Apr-15
NDVI
Precipitation
Month

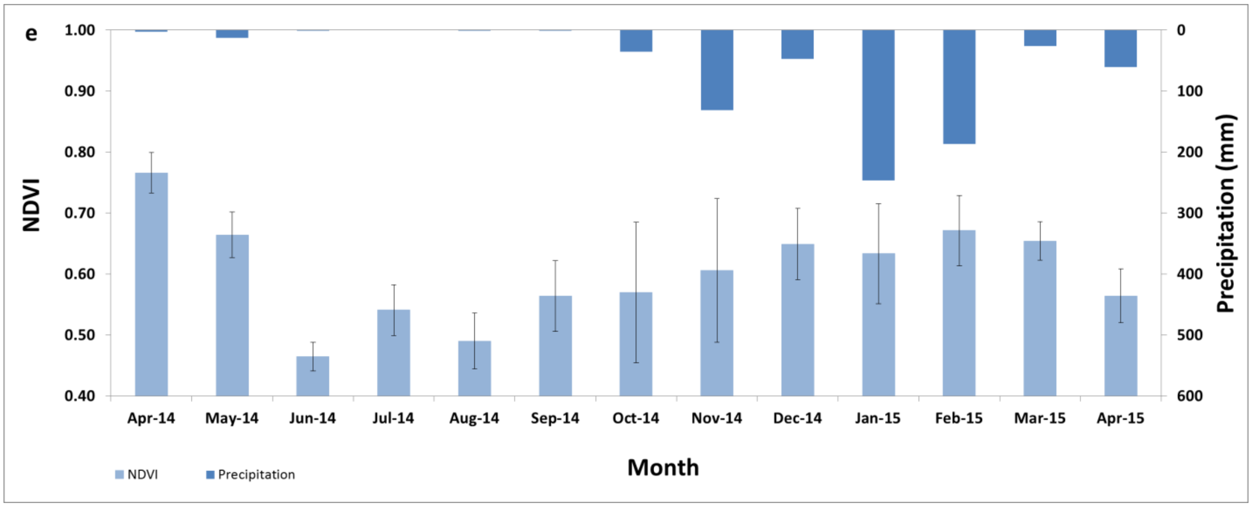

Fig. 12. Monthly NDVI and water potential for (a) the plot scale; and for (b) *P. latifolia*; (c) *O. europaea*; (d) *Q. calliprinos*; (e) *P. lentiscus*..

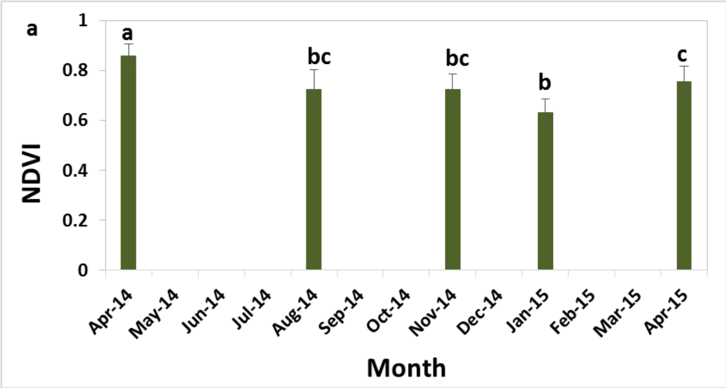

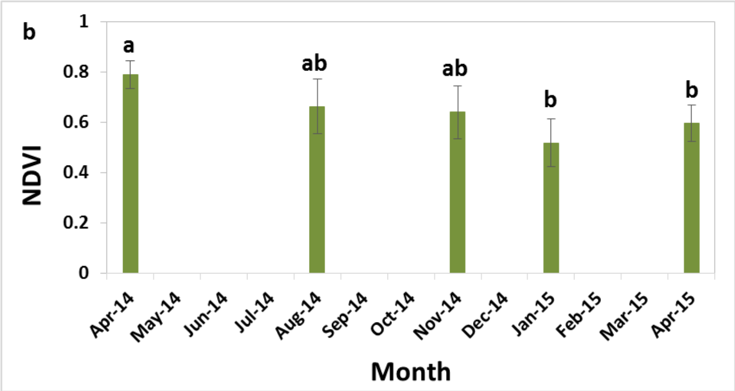

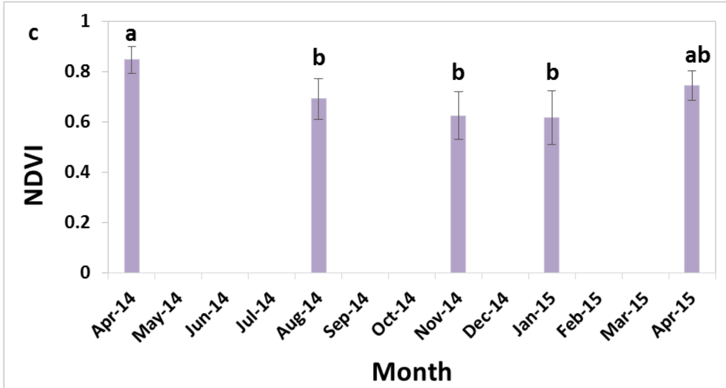

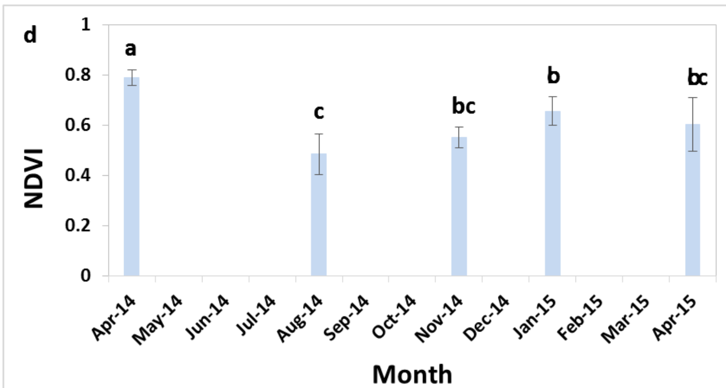

Fig. 13. Seasonal NDVI for (a) *P. latifolia*; (b) *O. europaea*; (c) *Q. calliprinos*; (d) *P. lentiscus.*

The physiological measurements reflected seasonal variation in water availability, in stomata aperture, and in chlorophyll concentration. In the summer season, water potential dropped significantly in all species, showing adjustments to water deficit in this season (Fig. 14.a-d). In comparison, during seasons where water availability was high, no significant differences were shown between the species (Fig. 14.e). Although physiological measurements showed response to summer drought in all species, there were some differences between them; *O. europaea* and *P. latifolia* reached to lower water potentials in comparison to *Q. calliprinos* and *P. lentiscus* (Fig. 15). Alongside, all species showed adjustments in their stomata regulation during the summer season, resulting in a reduced stomata conductance (Fig. 16). The variance in this measurement was very high (Fig. 16), presenting a difficulty in getting representative and reliable measurement. Total chlorophyll (a+b) concentrations in all species reached to their highest values during winter to spring seasons, and to their lowest values in the summer season (Fig. 17).

The phenological trends observed from the monthly time series of NDVI (Fig. 12), did not correspond directly with the physiological measurements in three of the observed species; minimal NDVI values for *P. latifolia, O. europaea* and *Q. calliprinos* were observed few months after the summer drought reflected by the low water potential values and reduced stomata conductance. Additionally, in the summer season, NDVI did not reflect the minimal chlorophyll concentrations that were measured. When all observations of chlorophyll concentration were regressed against NDVI or red reflectance values, no significant correlation was found (Fig. 18). The phenological trend of *P. lentiscus* was the only species that showed an agreement with the chlorophyll concentrations that were measured.

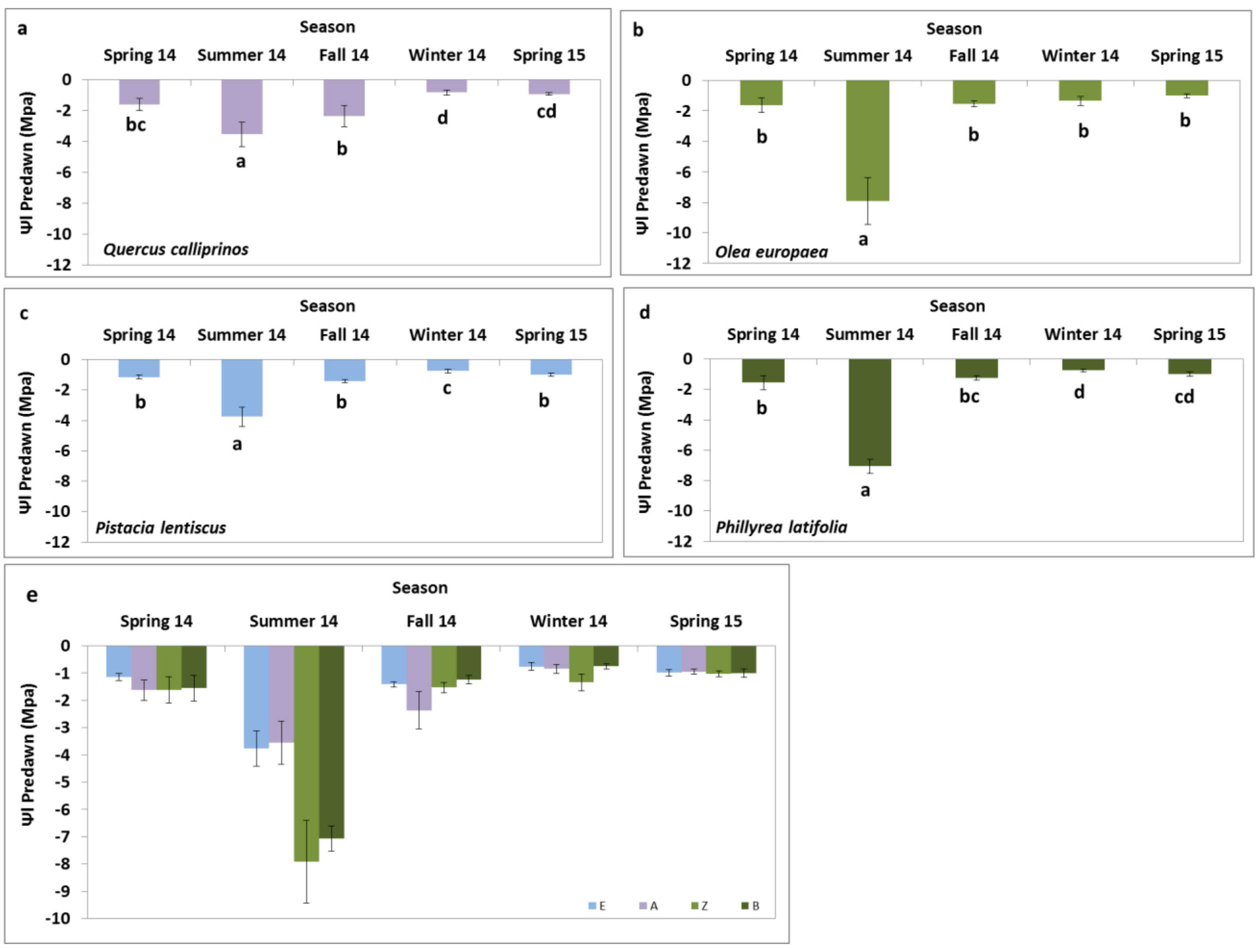

Fig. 14. Predawn water potential results for four monitored species along the seasons.

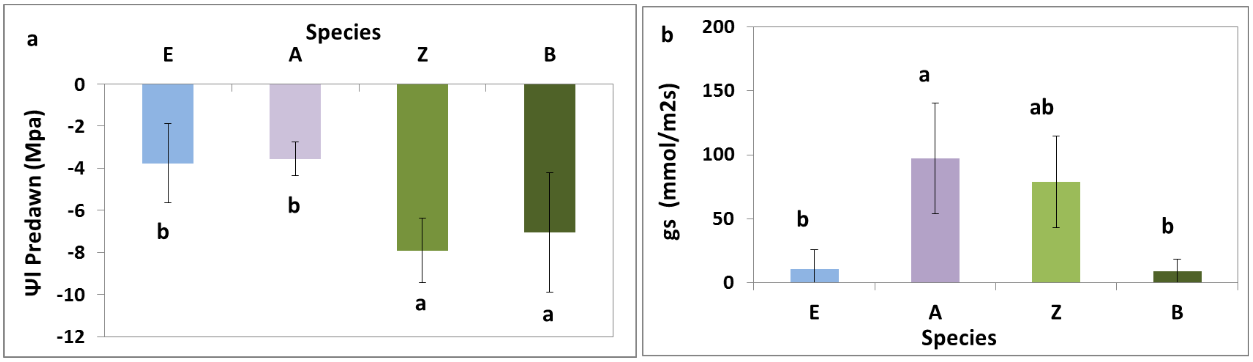

Fig. 15. (a) Predawn summer water potential; and (b) Midday stomata conductance results for four monitored species. Abbreviations: E- *P. lentiscus*, B- *P. latifolia*, Z- *O. europaea*, A- *Q. calliprinos*.

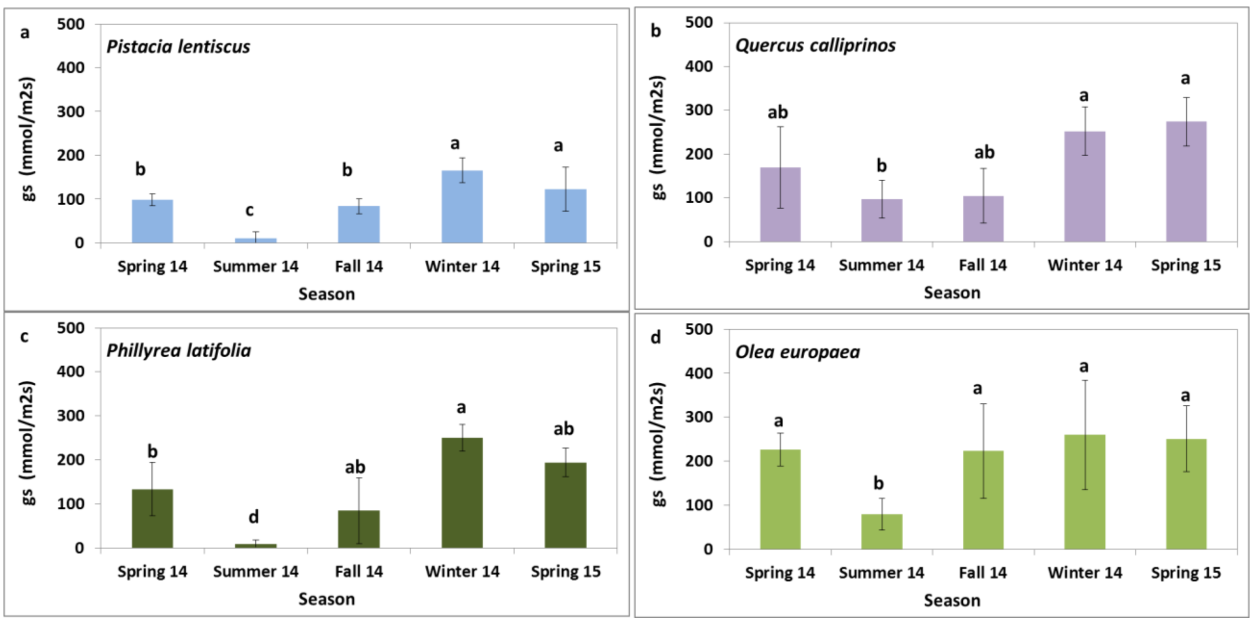

Fig. 16. Midday stomata conductance results for four monitored species.

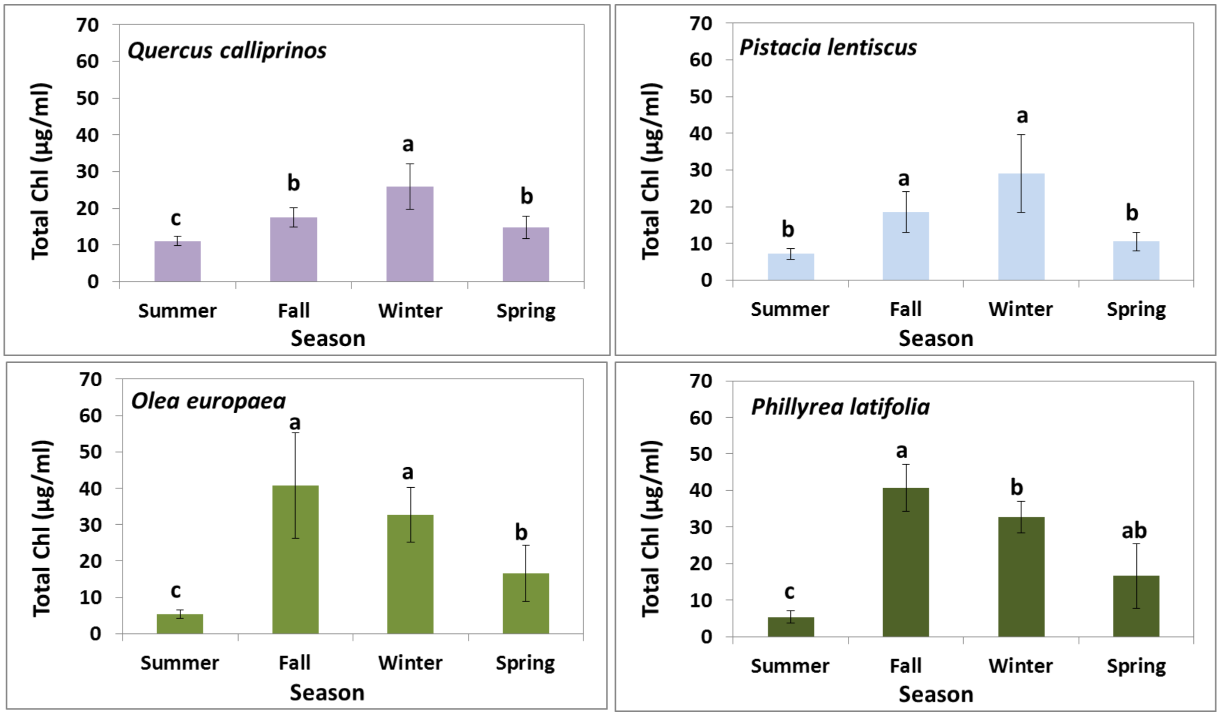

Fig. 17. Total chlorophyll (a+b) concentration results for four monitored species.

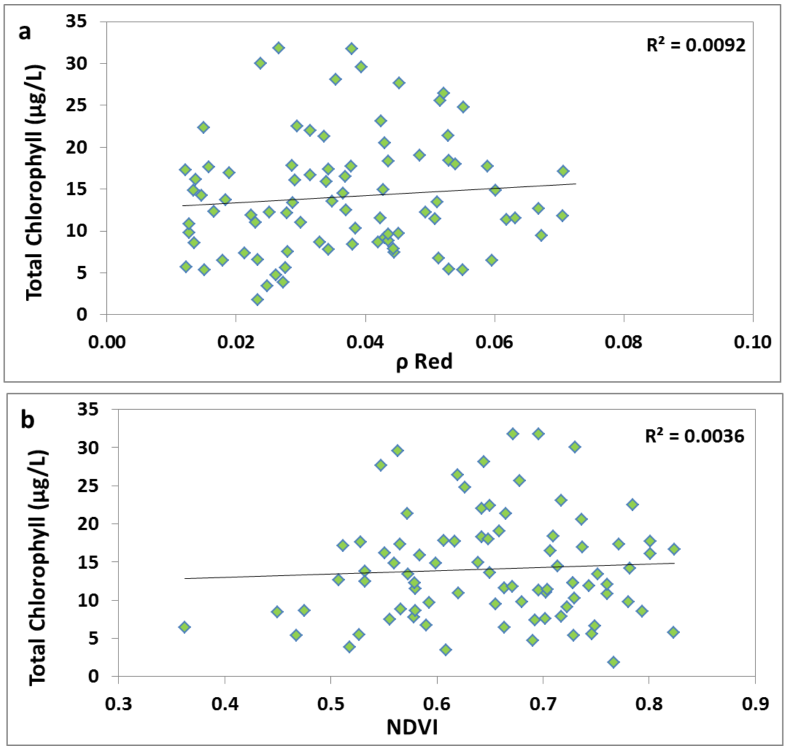

Fig. 18. Correlation between total chlorophyll (a+b) content with (a) red reflectance; (b) NDVI values.

4. Discussion

Results from time series analysis showed that generally NDVI had higher correlation with all of the climatic variables than NDWI. Moreover, the maximal correlation of both indices occurred approximately at the same time (PMA and lag components were similar). Although both indices were previously used for monitoring vegetation response to climate events (Anderson et al., 2010; Carcinoid et al., 2010; Gu et al., 2007), it seems that for the purpose of phenological modeling, NDVI is more suitable. These indices are sensitive to different aspects in the physiology of plants. NDVI is more correlated to photosynthetic activity, chlorophyll content and LAI, while NDWI is more sensitive to canopy water content, therefore it is possible that other climatic variables could better explain the variance in NDWI. Such variables could be environmental factors that affect the water status of plants, for instance, water content in the soil or vapor pressure deficit. From physiological point of view, it is highly probable that an initial response of NDWI will be distinguished first, indicating the existence of water stress in the summer time. On the other hand, since histological changes occur only after a reduction in leaf water content, a delayed decline in NDVI values is expected. In order to track this kind of response, different analyses should have been applied, such as tracing and comparing the timing of a specific phenological event using both indices. Although the analysis aimed mainly to explain the phenology of these forests, and not to focus on a specific phenological event, it can be a topic for future studies.

Various responses of phenology to climatic variables were shown, reflecting a changing sensitivity to climate with the transition from one climatic zone to another. When the correlation between VIs and precipitation was examined, it was found that the summed precipitation in the last of 3-4 months (in three southern sites) or with 5 months precipitation with a certain time lag (in the Galilee forest) produced the highest correlations. The findings from the three southern sites are in agreement with other studies (Davenport & Nicholson, 1993; Herrmann, Anyamba, & Tucker, 2005) that showed maximal response of NDVI to similar summation period. These findings show that the effect of climatic factors on phenology is accumulated with time, i.e., a certain amount of water should be absorbed by the soil and trees in order to motivate phenological responses (such as an increase in greenness). Alternatively, a certain duration of dry spell and high temperature, inhibits vegetative growth and decreases the greenness of the area. The fact that the influential PMA time scale of precipitation was increased with the transition from southern (2.5 months) to the northern site (5.5 months) can be attributed to diminishing role of water storage in the southern sites (Dorman, Perevolotsky, Sarris, & Svoray, 2015b). Although this research explored the effect of precipitation on tree growth, this parameter is closely related to the phenological cycle of trees. It demonstrated that in such dry areas, the influential rainfall scales are shortened, as the potential for water to be stored and carried over from one year to the next is low, due to very negative water balance which leads to loss of most of the annual rainfall during the same year (Dorman et al., 2015b). As a result in these dry sites, where water availability is low, phenological cycles are driven by short term precipitation periods

The results showed that the importance of precipitation anomaly differed between the sites (Table 2); its influence on phenology was reduced with the climatic gradient. In the northern sites the average precipitation is high enough to ensure functioning of the forest even under anomalous conditions. On the other hand, in the southern sites deviations from the average show immediate impacts. This finding can be explained as well by the lower accessibility of the southern site to deep water storage. As a result, the precipitation regime is a crucial factor in determining the phenology of these forests. Another interesting finding was the decreasing correlation between NDVI and NDWI from south to north (Fig. 9), indicating that in the northern site the water content is close to its maximal capacity, and therefore does not function as a limiting factor to the forest's greenness. The range of NDVI values shown under the same low NDWI values (Fig. 9) might be related to different physiological adaptations of trees to water stress conditions. It seems that under very low water content (expressed by low NDWI) forests in the northern sites manage to retain higher productivity (expressed by higher NDVI) relatively to the southern sites. In the transition from semi-arid climatic zone to humid zone the annual amount of precipitation can differ up to 550 mm. These differences in the available amount of water between the sites can explain the fact that precipitation was a weaker limiting factor in the northern sites. The studied forests differ also in their species composition; Yatir forest is mainly a monoculture *P. halepensis* forest, while other sites were more heterogeneous forests. The phenology of Mediterranean coniferous forests is mainly driven by water availability (Kramer et al., 2000), especially the phenology of forests that are situated in arid areas (S. M. Vicente-Serrano, 2007). Although *P. halepensis* is considered a resistant species to water stress (Atzmon, Moshe, & Schiller, 2004), the results indicate that its phenology dictated mainly by precipitation. In comparison to Yatir site, precipitation became equivalent or minor factor relative to temperature or radiation in others sites. Temperature is another major factor controlling the phenology of tree species (Morin, Roy, Sonié, & Chuine, 2010), and it is highly correlated with radiation. It is possible that in the northern sites, where precipitation amount is higher, temperature and radiation are stronger phenological triggers. Other site characteristics such as: the age of trees, their density, the lithology, the topography, can influence the functioning of these ecosystems, and their response to climatic variables. In order to quantify the influence of these factors, the spatial resolution of the analysis should be improved, thereby allowing capturing the variance in these variables.

VIs time series showed an annual cycle in all sites. This was supported by high correlations (Adj.R^2 of 0.5-0.7) between NDVI and the annual cycle component. Adding the anomaly of climatic variables produced models with high explanatory power. This indicates that much of the deviation of NDVI from its cycle could be explained by the deviation of climatic variables from their cycle, i.e. the anomaly in climatic variables clearly affects the anomaly of NDVI. As an explanatory model, this statistical modeling approach performed pretty well. However, examining the results from the validation period raised some challenges to the model performance for prediction purposes. The variability in the prediction ability between the sites can be attributed to two main reasons. Firstly, the occurrence of influential environmental events such as: fires, pest outbreaks and human intervention (pruning trees and diluting their density), were not considered in the model. This type of events can have a large scale influence on forest performance and greenness. Secondly, it is possible that a specific training period should have been fitted to each site. This direction should be further studied in order to define criteria to the choice of training period duration.

Results showed low predictive performance in years of unique climatic conditions; for instance, the last year of prediction showed large deviation from the measured data in all sites. This winter of 2014 was characterized by an uneven distribution of rain events, with two intense rain periods. Such events increase the runoff, decrease infiltration of the water to the soil, and therefore minimize the assimilation of water by the roots (Trenberth, 2011). Moreover, it might cause long term effects by intensifying soil erosion by runoff (Ziadat & Taimeh, 2013). In this year, which can be considered as a disturbance year, the prediction ability was tested under conditions that were quite different from those that were presented during the learning period. The annual distribution of rainfall in the learning period was more close to normal, and did not include years with such intense rain events. Although anomalies are taken into account in this model, it seems that they are not capturing the effect of such events, due to PMA time scale. PMA sums the precipitation for a period of three to five months, thus it is not able to express the distribution of precipitation along the rainy season. It was demonstrated (Dorman, Perevolotsky, Sarris, & Svoray, 2015a) that in semi-arid regions, it is important to take into account not only the annual rain amount but also other factors that quantify the effect of rainfall intensity, the proportion of large rain events, and the dry season length. Specifically in Yatir site, it can be seen that in the validation period the model overestimated NDVI in most of the period. The lower NDVI that was observed in this period might be due to the sequence of drought years occurring before and within the validation period. Each drought event influences not only on the current year, but might have implications on the coming years, as both the initiation of needle primordia and elongation of needles are affected by the availability of water (Kramer et al., 2000). A sequence of dry years might have a more complex effect on the phenology of forest, eventually expressed in lower NDVI values for several years. Moreover tree mortality occurred in several locations within these sites (Dorman, Svoray, Perevolotsky, et al., 2013; Ungar et al., 2013), and can have substantial effect on the mean regional NDVI. The limitations of the model that were considered here may be overcome by considering additional variables such as the number of rainy days, the distribution of the precipitation and the duration of the droughts (or excess precipitation periods).

Phenological monitoring in Ramat Hanadiv site showed annual cycles of four monitored evergreen tree and shrub species, and also an annual cycle for the plot scale level. Some of the observed changes in NDVI in the plot scale, can be attributed to the presence of herbaceous annual plants that contribute to higher NDVI values in the spring time. The monthly NDVI values for the four species were characterized by high variance. It is important to consider the fact that this research was conducted in a natural site, and not under a controlled environment, thus it reasonable to have some variation in the phenological cycle, even within the same species. This variance can be also effected from changes in microclimate conditions, or from species gender in the case of *P. lentiscus*. The phenology of all species was shown to be dictated by water availability. Although the vegetative growth occurred in different timings for each species, in all cases the rise in NDVI values occurred after a certain time lag from the beginning of rainy season. These findings are in correspondence with other researches that showed the phenology of Mediterranean trees is dictated mainly by water availably (Kramer et al., 2000). Specifically in Ramat HaNadiv, the general pattern and the fluctuations of the phenology of *Philerya* trees was found to be mainly regulated by water availability (Pollak et al., 2001). Minimal NDVI values for three tree species were shown around December 2014, after the long dry spell of the summer. Differently from these tree species, *P. lentiscus* shrubs showed minimal NDVI values already during summer season. In *P. lentiscus* grown under Meditterenean field conditions, leaf senescence, which is followed by abscission usually occurs in the summer (Diamantoglou & Kull, 1988).

Physiological measurements described water relations in individual trees and showed different responses to drought conditions occurring in the summer season. This was expressed in low water potentials of *O. europaea* and *P. latifolia* relatively to *Q. calliprinos* and *P. lentiscus*. Stomata closure as a result of water stress was regulated more strictly in *Q. calliprinos* and *O. europaea* relatively to *P. latifolia* and *P. lentiscus*. Although some variations were shown in the physiological response to water stress, it seems that the three tree species were able to retain relatively high NDVI values during the summer period. This characteristic of Mediterranean evergreen species is possible due to their adjustment to local climate through the development of deep root system (Canadell, 1996; Castro-D´ıez & Montserrat-Mart´ı, 1998).

The low correlations of total chlorophyll concentrations with NDVI are probably a result of an unrepresentative sampling procedure (only one representative branch was sampled form each tree). In evergreen trees, where leaves from different ages can be a part of the same canopy, it is important to try to model the amount of young and old leaves and to represent it correctly in the sample. Therefore, it is highly recommended to increase the number of samples. Additionally, it was previously shown (Zarco-Tejada, Miller, Morales, Berjón, & Agüera, 2004) that spectral indices do not show the same performance in tracking chlorophyll concentrations at the leaf and the canopy levels, due to the effect of scene components, such as soil and shadows. Moreover, Sun-exposed and shaded leaves have been shown to exhibit considerable physiological and morphological differences (Castro & Sanchez-Azofeifa, 2008). In the current study, these effects were partly considered by choosing manually the lighted parts of the tree for the analysis, and in most cases trees with dense canopies were chosen. An improvement can be achieved by using image classification as a preprocessing step. This might minimize the variability associated with the effects of shading and soil background, and result in more pronounced phenological cycles.

Additional important directions for further research are recommended. The first is including field phenological observations that will allow correlating the timing of phenological events derived from NDVI time series with those observed in the field. Combination of physiological measurements with phenological observations will allow explaining the cycles not only in regard to the physiological state of trees but also to their pheno-phases. The second is the low performance of the camera in clouded and dark days (especially in the winter months). In the spring and summer months the images were mainly bright and clear. Starting from the September, images became darkened due to low exposure adjusted by the automatic mode. The third is the reliability of reflectance values in clouded days. The site is located close to a marine area, therefore the amount of cloudy days is relatively high. As the camera is located about 200 m from the monitored slope, it is possible that under cloudy conditions the down-welling radiation gathered by the ILS, is not the same as in the monitored area. This might cause to a biased reflectance values, therefore, such affects have to be quantitatively evaluated. The fourth is the essential need for automated image processing procedure in order to create continuous VIs data. In the long term, such data will allow quantifying the relations between climatic variables and spectral VI, and provide an understating of how climate changes affect Mediterranean ecosystems.

5. Conclusions

Time series analysis was implemented on phenological record of the last 15 years in four forests located along a climatic gradient in Israel. This analysis quantified the relations between the phenology of these forests (in the form of spectral vegetation indices) and three main climatic variables. In accordance with the hypothesis, this analysis revealed that the relative influence of precipitation is decreasing from south to north, and the duration of the most influential precipitation period is increasing, indicating on the diminishing role of moisture stored in deep soil layers. However, the hypothesis of precipitation anomaly being the main driver of phenology in all sites was rejected. These findings show that the phenology of the studied forests is sensitive to the existing variations in climate in Israel. Contrary to the hypothesis, both VI's showed similar relations with climatic variables. NDVI was slightly more correlated with climatic variables than NDWI, thus suggesting that it is more suitable for phenological modeling using these specific climatic variables. The explanatory models that were created on the basis of this analysis showed a relatively high explanatory power, and a reasonable predictive skill. Specifically, it was shown that the predictive performance of the model in years with extreme climatic events is lower. Climate predictions show that the frequency of such events is expected to increase (IPCC, 2014); therefore, it is highly important to have reliable models that will indicate how forest phenology will respond to future climate scenarios. The fact that these models were implemented on forests that lay across a climatic gradient, extends their relevance to various regions across the Mediterranean, therefore it is worthy to study them further. Improvements can be achieved by transition to a more complex modeling approach that takes additional biotic and abiotic factors into account. Additionally, it is important to represent not only the accumulated effect of climatic variables, but also their distribution in time and additional characteristics of their variability. Results from one year of monitoring in Ramat HaNadiv site showed distinct phenological cycles of the dominant tree and shrub species. It seems that the phenology of these species is dictated by the water availability in this area, and the rise in NDVI values occurs after similar precipitation summing period as was detected in the forested areas. Several methodological directions regarding the automated processing of the data and image classification remained open and require further research. In summary, the use of VI's time series for both monitoring and modeling purposes has shown promising results that might be implemented for ecosystems monitoring and climate change influence assessment.

6. References

Allen, C. D., Macalady, A. K., Chenchouni, H., Bachelet, D., McDowell, N., Vennetier, M., … Cobb, N. (2010). A global overview of drought and heat-induced tree mortality reveals emerging climate change risks for forests. *Forest Ecology and Management*, *259*(4), 660–684. http://doi.org/10.1016/j.foreco.2009.09.001

Anderson, L. O., Malhi, Y., Aragão, L. E. O. C., Ladle, R., Arai, E., Barbier, N., & Phillips, O. (2010). Remote sensing detection of droughts in Amazonian forest canopies. *New Phytologist*, *187*(3), 733–750. http://doi.org/10.1111/j.1469-8137.2010.03355.x

Atzmon, N., Moshe, Y., & Schiller, G. (2004). Ecophysiological response to severe drought in Pinus halepensisMill. trees of two provenances. *Plant Ecology*, *171*, 15–22.

Becker-Reshef, I., Justice, C., Sullivan, M., Vermote, E., Tucker, C., Anyamba, A., … Doorn, B. (2010). Monitoring Global Croplands with Coarse Resolution Earth Observations: The Global Agriculture Monitoring (GLAM) Project. *Remote Sensing*, *2*(June), 1589–1609. http://doi.org/10.3390/rs2061589

Beurs Kirsten M.de, & Henebry, G. M. (2010). *Phenological Research*. *Media*. http://doi.org/10.1007/978-90-481-3335-2

Canadell, J. (1996). Maximum rooting depth of vegetation types at the global scale. *Oecologia*, *108*, 583–595. http://doi.org/10.1007/BF00329030

Carcinoid, R., Liver, M., Nodes, L., Metastases, B., & Responded, T. (2010). Evaluating MODIS vegetation and water indices for detecting canopy stress during the 2005 drought in Amazonia, 2349–2351.

Castro, K. L., & Sanchez-Azofeifa, G. A. (2008). Changes in Spectral Properties, Chlorophyll Content and Internal Mesophyll Structure of Senescing Populus balsamifera and Populus tremuloides Leaves. *Sensors*, *8*(1), 51–69. http://doi.org/10.3390/s8010051

Castro-D´ıez, P., & Montserrat-Mart´ı, G. (1998). Phenological pattern of fifteen Mediterranean phanaerophytes from Quercus ilex communities of NE-Spain. *Plant Ecology*, *139*, 103–112. http://doi.org/10.1023/A

Chuine, I. (2000). A unified model for budburst of trees. *Journal of Theoretical Biology*, *207*(3), 337–347. http://doi.org/10.1006/jtbi.2000.2178

Churkina, G., Schimel, D., Braswell, B. H., & Xiao, X. (2005). Spatial analysis of growing season length control over net ecosystem exchange. *Global Change Biology*, *11*(10), 1777–1787. http://doi.org/10.1111/j.1365-2486.2005.001012.x

Cleland, E. E., Chiariello, N. R., Loarie, S. R., Mooney, H. a, & Field, C. B. (2006). Diverse responses of phenology to global changes in a grassland ecosystem. *Proceedings of the National Academy of Sciences of the United States of America*, *103*(37), 13740–4. http://doi.org/10.1073/pnas.0600815103

Connor, O., Dwyer, N., & Cawkwell, F. (2008). Satellite remote sensing as a tool for monitoring vegetation seasonality. In *Proceedings of the remote sensing and photogrammetry society conference* (pp. 15–17).

Cook, B. I., Smerdon, J. E., Seager, R., & Coats, S. (2014). Global warming and 21st century drying. *Climate Dynamics*, *43*, 2607–2627. http://doi.org/10.1007/s00382-014-2075-y

Crimmins, M. a, & Crimmins, T. M. (2008). Monitoring plant phenology using digital repeat photography. *Environmental Management*, *41*(6), 949–58. http://doi.org/10.1007/s00267-008-9086-6

Currit, N., & St Clair, S. B. (2010). Assessing the impact of extreme climatic events on aspen defoliation using MODIS imagery. *Geocarto International*, *25*(2), 133–147. http://doi.org/10.1080/10106040903051975

Davenport, M. L., & Nicholson, S. E. (1993). On the relation between rainfall and the Normalized Difference Vegetation Index for diverse vegetation tpes in East Africa. *International Journal of Remote Sensing*. http://doi.org/10.1080/01431169308954042

Diamantoglou, S., & Kull, U. (1988). Seasonal variations of nitrogen com ponents in Mediterranean evergreen sclerophyllous leaves. *Flora*, *180*, 377–390.

Dorman, M., Perevolotsky, A., Sarris, D., & Svoray, T. (2015a). Amount vs. temporal pattern: On the importance of intra-annual climatic conditions on tree growth in a dry environment. *Journal of Arid Environments*, *118*, 65–68. http://doi.org/10.1016/j.jaridenv.2015.03.002

Dorman, M., Perevolotsky, A., Sarris, D., & Svoray, T. (2015b). The effect of rainfall and competition intensity on forest response to drought: lessons learned from a dry extreme. *Oecologia*, *177*(4), 1025–38. http://doi.org/10.1007/s00442-015-3229-2

Dorman, M., Svoray, T., & Perevolotsky, A. (2013). Homogenization in forest performance across an environmental gradient - The interplay between rainfall and topographic aspect. *Forest Ecology and Management*, *310*, 256–266. http://doi.org/10.1016/j.foreco.2013.08.026

Dorman, M., Svoray, T., Perevolotsky, A., & Sarris, D. (2013). Forest performance during two consecutive drought periods: Diverging long-term trends and short-term responses along a climatic gradient. *Forest Ecology and Management*, *310*, 1–9. http://doi.org/10.1016/j.foreco.2013.08.009

Eamus, D. (1999). Ecophysiological traits of deciduous and evergreen woody species in the seasonally dry tropics. *Trends in Ecology and Evolution*, *14*(1), 11–16. http://doi.org/10.1016/S0169-5347(98)01532-8

Estiarte, M., & Peñuelas, J. (2015). Alteration of the phenology of leaf senescence and fall in winter deciduous species by climate change: effects on nutrient proficiency. *Global Change Biology*, *21*(3), 1005–1017. http://doi.org/10.1111/gcb.12804

Ganguly, S., Friedl, M. a., Tan, B., Zhang, X., & Verma, M. (2010). Land surface phenology from MODIS: Characterization of the Collection 5 global land cover dynamics product. *Remote Sensing of Environment*, *114*(8), 1805–1816. http://doi.org/10.1016/j.rse.2010.04.005

Gao, B. C. (1996). NDWI - A normalized difference water index for remote sensing of vegetation liquid water from space. *Remote Sensing of Environment*, *58*(3), 257–266. http://doi.org/10.1016/S0034-4257(96)00067-3

Garonna, I., De Jong, R., De Wit, a J. W., Mücher, C. a, Schmid, B., & Schaepman, M. (2014). Strong contribution of autumn phenology to changes in satellite-derived growing season length estimates across Europe (1982-2011). *Global Change Biology*, n/a–n/a. http://doi.org/10.1111/gcb.12625

Graham, E. a., Riordan, E. C., Yuen, E. M., Estrin, D., & Rundel, P. W. (2010). Public Internet-connected cameras used as a cross-continental ground-based plant phenology monitoring system. *Global Change Biology*, no–no. http://doi.org/10.1111/j.1365-2486.2010.02164.x

Gu, Y., Brown, J. F., Verdin, J. P., & Wardlow, B. (2007). A five-year analysis of MODIS NDVI and NDWI for grassland drought assessment over the central Great Plains of the United States. *Geophysical Research Letters*, *34*(6), L06407. http://doi.org/10.1029/2006GL029127

Hasselquist, N. J., Allen, M. F., & Santiago, L. S. (2010). Water relations of evergreen and drought-deciduous trees along a seasonally dry tropical forest chronosequence. *Oecologia*, *164*(4), 881–890. http://doi.org/10.1007/s00442-010-1725-y

Herrmann, S. M., Anyamba, A., & Tucker, C. J. (2005). Recent trends in vegetation dynamics in the African Sahel and their relationship to climate. *Global Environmental Change*, *15*(4), 394–404. http://doi.org/10.1016/j.gloenvcha.2005.08.004

Hufkens, K., Friedl, M., Sonnentag, O., Braswell, B. H., Milliman, T., & Richardson, A. D. (2012). Linking near-surface and satellite remote sensing measurements of deciduous broadleaf forest phenology. *Remote Sensing of Environment*, *117*, 307–321. http://doi.org/10.1016/j.rse.2011.10.006

Hunter, F. A., & Lechowicz, J. M. (1992). Predicting the Timing of Budburst in Temperate Trees. *Journal of Applied Ecology*, *29*(3), 597–604.

IPCC. (2014). *Climate Change 2014: Synthesis Report. Contribution of Working Groups I, II and III to the Fifth Assessment Report of the Intergovernmental Panel on Climate Change[Core Writing Team, R.K. Pachauri and L.A. Meyer (eds.)]*. Geneva, Switzerland.

Ji, L., Zhang, L., Wylie, B. K., & Rover, J. (2011). On the terminology of the spectral vegetation index (NIR − SWIR)/(NIR + SWIR). *International Journal of Remote Sensing*, *32*(21), 6901–6909. http://doi.org/10.1080/01431161.2010.510811

Johnston, A., & Reekie, E. (2008). REGARDLESS OF WHETHER RISING ATMOSPHERIC CARBON DIOXIDE LEVELS INCREASE AIR TEMPERATURE , FLOWERING PHENOLOGY WILL BE AFFECTED. *Int. J. Plant Sci.*, *169*(9), 1210–1218. http://doi.org/10.1086/591978

Jolly, W. M., Nemani, R., & Running, S. W. (2005). A generalized, bioclimatic index to predict foliar phenology in response to climate. *Global Change Biology*, *11*(4), 619–632. http://doi.org/10.1111/j.1365-2486.2005.00930.x

Julitta, T., Cremonese, E., Migliavacca, M., Colombo, R., Galvagno, M., Siniscalco, C., … Menzel, A. (2014). Agricultural and Forest Meteorology Using digital camera images to analyse snowmelt and phenology of a subalpine grassland. *Agricultural and Forest Meteorology*, *198-199*, 116–125. http://doi.org/10.1016/j.agrformet.2014.08.007

Kafle, H. K., & Bruins, H. J. (2009). Climatic trends in Israel 1970–2002: warmer and increasing aridity inland. *Climatic Change*, *96*(1-2), 63–77. http://doi.org/10.1007/s10584-009-9578-2

Kramer, K., Leinonen, I., & Loustau, D. (2000). The importance of phenology for the evaluation of impact of climate change on growth of boreal, temperate and Mediterranean forests ecosystems: an overview. *International Journal of Biometeorology*, *44*(2), 67–75. http://doi.org/10.1007/s004840000066

Kuster, T. M., Dobbertin, M., Günthardt-Goerg, M. S., Schaub, M., & Arend, M. (2014). A phenological timetable of oak growth under experimental drought and air warming. *PLoS ONE*, *9*(2). http://doi.org/10.1371/journal.pone.0089724

Lhermitte, S., Verbesselt, J., Jonckheere, I., Nackaerts, K., van Aardt, J. a. N., Verstraeten, W. W., & Coppin, P. (2008). Hierarchical image segmentation based on similarity of NDVI time series. *Remote Sensing of Environment*, *112*(2), 506–521. http://doi.org/10.1016/j.rse.2007.05.018

Li, D., Liu, H., Qiao, Y., Wang, Y., Cai, Z., Dong, B., … Liu, M. (2013). Effects of elevated CO2 on the growth, seed yield, and water use efficiency of soybean (Glycine max (L.) Merr.) under drought stress. *Agricultural Water Management*, *129*, 105–112. http://doi.org/10.1016/j.agwat.2013.07.014

Lichtenthaler, H. K., & Buschmann, C. (2001). Chlorophylls and Carotenoids : Measurement and Characterization by UV-VIS. *Current Protocols in Food Analytical Chemistry*, *F4.3.1-F4.*(Supplement 1), 1–8. http://doi.org/10.1002/0471142913

Luedeling, E., Guo, L., Dai, J., Leslie, C., & Blanke, M. M. (2013). Differential responses of trees to temperature variation during the chilling and forcing phases. *Agricultural and Forest Meteorology*, *181*, 33–42. http://doi.org/10.1016/j.agrformet.2013.06.018

Ma, X., Huete, A., Yu, Q., Coupe, N. R., Davies, K., Broich, M., … Eamus, D. (2013). Spatial patterns and temporal dynamics in savanna vegetation phenology across the North Australian Tropical Transect. *Remote Sensing of Environment*, *139*, 97–115. http://doi.org/10.1016/j.rse.2013.07.030

Misson, L., Degueldre, D., Collin, C., Rodriguez, R., Rocheteau, A., Ourcival, J. M., & Rambal, S. (2011). Phenological responses to extreme droughts in a Mediterranean forest. *Global Change Biology*, *17*(2), 1036–1048. http://doi.org/10.1111/j.1365-2486.2010.02348.x

Morin, X., Roy, J., Sonié, L., & Chuine, I. (2010). Changes in leaf phenology of three European oak species in response to experimental climate change. *The New Phytologist*, *186*(4), 900–910. http://doi.org/10.1111/j.1469-8137.2010.03252.x

Morisette, J. T., Richardson, A. D., Knapp, A. K., Fisher, J. I., Graham, E. a, Abatzoglou, J., … Liang, L. (2009). Tracking the rhythm of the seasons in the face of global change: phenological research in the 21st century. *Frontiers in Ecology and the Environment*, *7*(5), 253–260. http://doi.org/10.1890/070217

Nagy, L., Kreyling, J., Gellesch, E., Beierkuhnlein, C., & Jentsch, a. (2013). Recurring weather extremes alter the flowering phenology of two common temperate shrubs. *International Journal of Biometeorology*, *57*(4), 579–88. http://doi.org/10.1007/s00484-012-0585-z

Nemani, R. R., Keeling, C. D., Hashimoto, H., Jolly, W. M., Piper, S. C., Tucker, C. J., … Running, S. W. (2003). Climate-driven increases in global terrestrial net primary production from 1982 to 1999. *Science (New York, N.Y.)*, *300*, 1560–1563. http://doi.org/10.1126/science.1082750

Norby, R. J., Hartz-rubin, J. S., & Verbrugge, M. J. (2003). Phenological resp onses in m aple to ex perime ntal atmospheric warming and CO 2 enrichment Phenological responses in maple to experimental atmospheric warming and CO 2 enrichment. *Global Change Biology*, *9*, 1792–1801. http://doi.org/10.1046/j.1529-8817.2003.00714.x

Ohana-Levi, N., Karnieli, A., Egozi, R., Givati, A., & Peeters, A. (2015). Modeling the Effects of Land-Cover Change on Rainfall-Runoff Relationships in a Semiarid , Eastern Mediterranean Watershed.

Osem, Y., Zangy, E., Bney-Moshe, E., Moshe, Y., Karni, N., & Nisan, Y. (2009). The potential of transforming simple structured pine plantations into mixed Mediterranean forests through natural regeneration along a rainfall gradient. *Forest Ecology and Management*, *259*(1), 14–23. http://doi.org/10.1016/j.foreco.2009.09.034

Parmesan Camille, & Gary, Y. (2003). A globally coherent fingerprint of climate change impacts across natural systems. *Nature*, *421*, 37.

Pollak, G., Swartz Tzahor, R., & Perevolotsky, A. (2001). The timing and magnitude of the phenological processes in Phillyrea Latifolia L. under Mediterranean conditions and disturbance regimes. *Ecology & Environment*, *6*, 156–168 (In Hebrew).

Richardson, A. D., Braswell, B. H., Hollinger, D. Y., Jenkins, J. P., & Ollinger, S. V. (2009). Near-surface remote sensing of spatial and temporal variation in canopy phenology. *Ecological Applications : A Publication of the Ecological Society of America*, *19*(6), 1417–28.

Richardson, A. D., Jenkins, J. P., Braswell, B. H., Hollinger, D. Y., Ollinger, S. V, & Smith, M.-L. (2007). Use of digital webcam images to track spring green-up in a deciduous broadleaf forest. *Oecologia*, *152*(2), 323–34. http://doi.org/10.1007/s00442-006-0657-z

Safriel, U. (2014). Desertification - local problem and global threats. *Ecology & Environment, 2,* 152–160 (in Hebrew).

Shahar, A. (1995). *New Israeli Atlas*. (A. Shahar, Ed.). Tel aviv: Israeli mapping center.

Sonnentag, O., Hufkens, K., Teshera-Sterne, C., Young, A. M., Friedl, M., Braswell, B. H., … Richardson, A. D. (2012). Digital repeat photography for phenological research in forest ecosystems. *Agricultural and Forest Meteorology*, *152*(1), 159–177. http://doi.org/10.1016/j.agrformet.2011.09.009

Trenberth, K. E. (2011). Changes in precipitation with climate change. *Climate Research*, *47*(1-2), 123–138. http://doi.org/10.3354/cr00953

Tucker, C. J. (1979). Red and Photographic Infrared Linear Combinations for Monitoring Vegetation. *Remote Sensing of Environment*, *8*(2), 127–150.

Ungar, E. D., Rotenberg, E., Raz-Yaseef, N., Cohen, S., Yakir, D., & Schiller, G. (2013). Transpiration and annual water balance of Aleppo pine in a semiarid region: Implications for forest management. *Forest Ecology and Management*, *298*, 39–51. http://doi.org/10.1016/j.foreco.2013.03.003

Vicente-Serrano, S., Cabello, D., Tomás-Burguera, M., Martín-Hernández, N., Beguería, S., Azorin-Molina, C., & Kenawy, A. (2015). Drought Variability and Land Degradation in Semiarid Regions: Assessment Using Remote Sensing Data and Drought Indices (1982–2011). *Remote Sensing*, *7*(4), 4391–4423. http://doi.org/10.3390/rs70404391

Vicente-Serrano, S. M. (2007). Evaluating the impact of drought using remote sensing in a Mediterranean, Semi-arid Region. *Natural Hazards*, *40*(1), 173–208. http://doi.org/10.1007/s11069-006-0009-7

Viskari, T. T., Hardiman, B., Desai, a. R., & Dietze, M. C. (2014). Model-data assimilation of multiple phenological observations to constrain and predict leaf area index. *In Review*, *25*(2), 546–558. http://doi.org/10.1890/14-0497.1

Vitasse, Y., François, C., Delpierre, N., Dufrêne, E., Kremer, A., Chuine, I., & Delzon, S. (2011). Assessing the effects of climate change on the phenology of European temperate trees. *Agricultural and Forest Meteorology*, *151*(7), 969–980. http://doi.org/10.1016/j.agrformet.2011.03.003

Volcani, a., Karnieli, a., & Svoray, T. (2005). The use of remote sensing and GIS for spatio-temporal analysis of the physiological state of a semi-arid forest with respect to drought years. *Forest Ecology and Management*, *215*(1-3), 239–250. http://doi.org/10.1016/j.foreco.2005.05.063

Williams, L. E., & Araujo, F. J. (2002). Correlations among Predawn Leaf , Midday Leaf , and Midday Stem Water Potential and their Correlations with other Measures of Soil and Plant Water Status in Vitis vinifera. *J Amer Soc Hort Sci.*, *127*(3), 448–454.

Zarco-Tejada, P. J., Miller, J. R., Morales, a., Berjón, a., & Agüera, J. (2004). Hyperspectral indices and model simulation for chlorophyll estimation in open-canopy tree crops. *Remote Sensing of Environment*, *90*(4), 463–476. http://doi.org/10.1016/j.rse.2004.01.017

Zelikova, T. J., Williams, D. G., Hoenigman, R., Blumenthal, D. M., Morgan, J. A., & Pendall, E. (2015). Seasonality of soil moisture mediates responses of ecosystem phenology to elevated CO 2 and warming in a semi-arid grassland. *Journal of Ecology*, 1119–1130. http://doi.org/10.1111/1365-2745.12440

Zhao, M. F., Peng, C. H., Xiang, W. H., Deng, X. W., Tian, D. L., Zhou, X. L., … Zhao, Z. H. (2013). Plant phenological modeling and its application in global climate change research: overview and future challenges. *Environmental Reviews*, *21*(1), 1–14. http://doi.org/10.1139/er-2012-0036

Zhou, Y., Zhang, L., Fensholt, R., Wang, K., Vitkovskaya, I., & Tian, F. (2015). Climate Contributions to Vegetation Variations in Central Asian Drylands: Pre- and Post-USSR Collapse. *Remote Sensing*, *7*(3), 2449–2470. http://doi.org/10.3390/rs70302449

Ziadat, F. M., & Taimeh, a. Y. (2013). Effect of rainfall intensity, slope, land use and antecedent soil moisture on soil erosion in an arid environment. *Land Degradation and Development*, *24*(6), 582–590. http://doi.org/10.1002/ldr.2239

7. Appendices

7.1 Technical recommendations for further work with MCA camera

1. Bands selection- In order to monitor the location of red edge position by the interpolation method (Eq. 8), additional band in the red spectral range is needed, preferably a band with central wavelength of 700 nm.

$$\lambda = 700 + 40 * \frac{((\rho 670 + \rho 780)/2) - \rho 700)}{(\rho 740 - \rho 700)} \quad (8)$$

2. Bands calibration- There is a need to make sure that the bands are well calibrated and that the relative exposure settings are adjusted according to the sensor sensitivity. In the current case all bands (except the master band) received 100% relative exposure. The correctness of this calibration needed to be checked in front of the company.
3. ILS calibration- as the operations of this component is still unclear for us, it is necessary to validate the reflectance data. This can be achieved by laboratory experiment, in which an image of an object and a white reference will be taken. It is important to make sure that the white reference and the ILS component are located in the same angle to the light source.
4. Geometrical correction- The quality of geometrical alignment carried out in the Pixel Wrench software was not satisfactory for our applications. The deviation between the bands reached to 2-3 pixels, whereas results from calibration in ERDAS software improved the deviation to about half a pixel. However, a lack of automated process in ERDAS software makes it very hard to work with large amount of data.
5. Storage box- The effect of used relatively thick glasses should be examined. Maybe it worthwhile to use thinner glasses. Additionally, it is very important to keep the glasses clean.

7.2 Additional Graphs

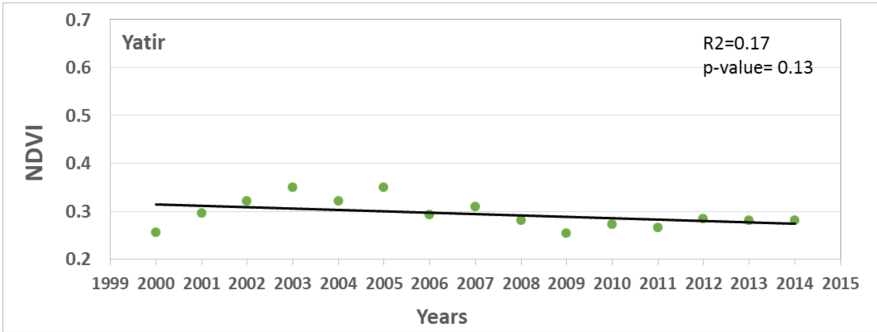

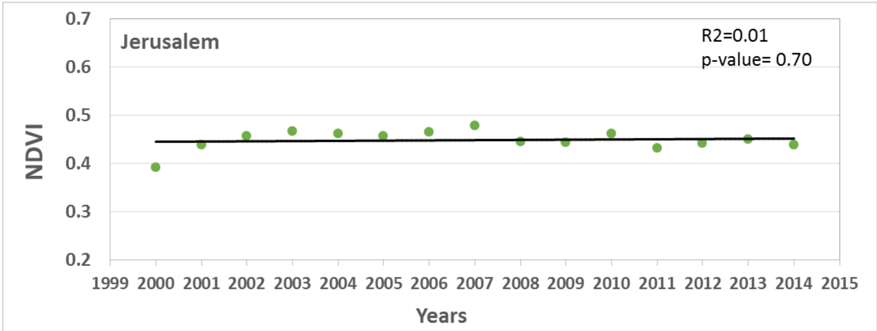

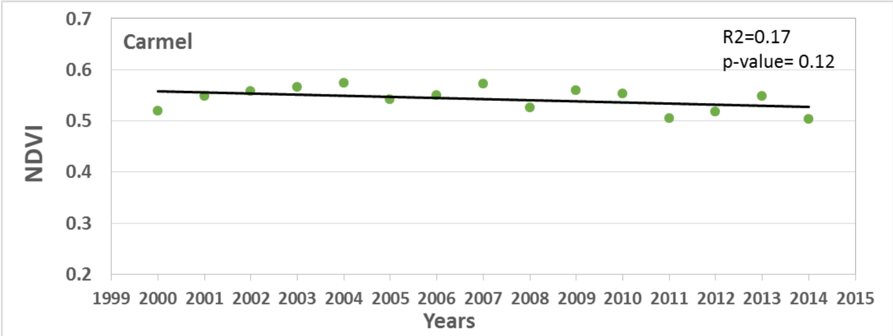

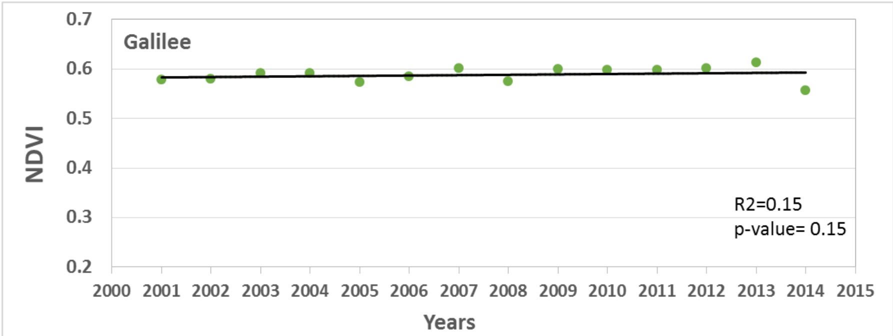

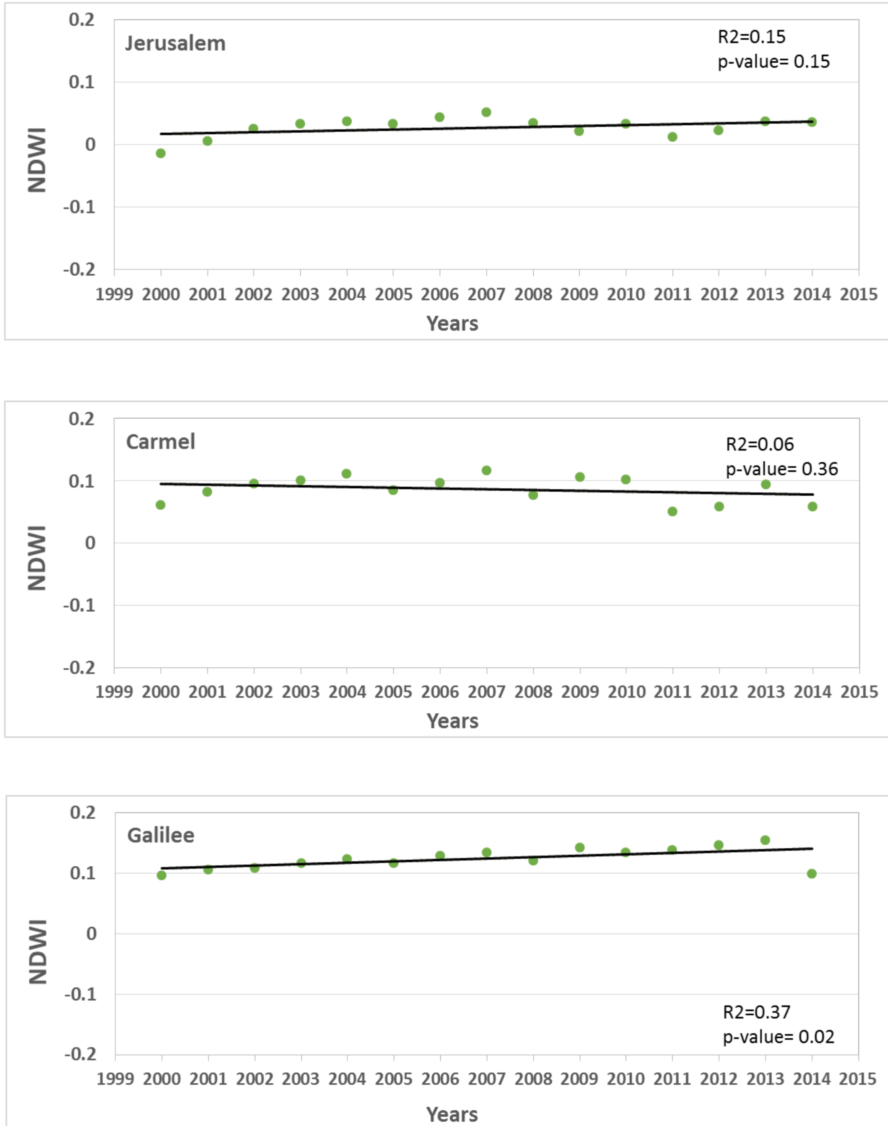

Fig. 19. Regression results between yearly mean VIs and time. There was no significant yearly time trend in VIs in all sites except in the NDWI of Galilee site.